Informed Data-Independent Acquisition Enables Targeted Quantification of Key Regulatory Proteins in Cell Fate Decision at Single-Cell Resolution

Jakob Woessmann [1,*], Valdemaras Petrosius [1], Sofie Schovsbo [2,3], Tabiwang N. Arrey [5], Benjamin Furtwängler [1], Jeff Op de Beeck [6], Eugen Damoc [5], Bo T. Porse [2,3,4,*], and Erwin M. Schoof [1,*]

1. Department of Biotechnology and Biomedicine, Technical University of Denmark, 2800 Kgs. Lyngby, Denmark
2. The Finsen Laboratory, Rigshospitalet, Faculty of Health Sciences, University of Copenhagen, 2200 Copenhagen, Denmark
3. Biotech Research and Innovation Centre, Faculty of Health Sciences, University of Copenhagen, Denmark
4. Department of Clinical Medicine, University of Copenhagen, Copenhagen, Denmark
5. Thermo Fisher Scientific (Bremen) GmbH, Bremen, Germany
6. Thermo Fisher Scientific, 9052 Gent, Belgium

* Corresponding authors

Abstract

Cellular differentiation processes are largely orchestrated by variation in transcription factor (TF) abundance. Since these proteins are usually expressed at extremely low levels, studying TF-driven cellular processes using single-cell proteomics by mass spectrometry (scp-MS) has been challenging. Here we present informed DIA (iDIA), an acquisition method tailored towards low-input and scp-MS. iDIA combines targeted and global proteomics in a single acquisition scheme and is by design universally applicable on different MS instrumentation. By combining wide window (ww)PRM scans with DIA acquisition, we observed a median 4-fold improvement in limit of quantification with targeted acquisitions, while maintaining biologically meaningful global proteome coverage. We utilize this gained sensitivity to quantify TFs in single murine hematopoietic stem and progenitor cells and showcase their lineage-specific regulation.

Introduction

Technical advances in single-cell proteomics by mass spectrometry (scp-MS) have recently led to impressive increases in proteome depth and sample throughput [1], [2], [3], [4]. Developments in sample preparation and multiplexing, liquid

chromatography (LC), and mass spectrometry (MS) have all contributed to improvements in global proteome coverage, which now has reached beyond 5,000 proteins per cell [2], [3], [4], [5], [6], [7], [8]. These developments have progressed hand in hand with a widespread adoption of label-free data-independent acquisition (DIA). However, addressing specific biological questions often requires reproducible quantification of key regulatory proteins, which are often low-abundant and therefore challenging to measure in scp-MS. Consequently, analyses such as MS-based quantification of transcription factors (TF) during hematopoietic stem and progenitor cells differentiation have, to our knowledge, mainly been demonstrated from nuclear extracts of millions of cells combined with targeted proteomics [9]. To truly be able to capture the TF dynamics governing lineage decisions in complex stem cell differentiation hierarchies, we need to be able to resolve the cell heterogeneity therein, making single-cell resolution essential. As mRNA levels frequently fail to correlate with functional protein abundance, especially in the most primitive stem cell compartment [10], protein-level measurements are particularly critical. To be able to capture both the TFs themselves, and their up- and downstream effectors, technology is needed that will allow us to resolve how specific regulators orchestrate fate choices with the precision and specificity that the biology demands, for which scp-MS is a prime candidate.

Targeted proteomics techniques such as parallel reaction monitoring (PRM) and Selected reaction monitoring (SRM) have been developed to quantify protein targets of interest with high specificity and sensitivity [11], [12]. So far only limited application of PRM in scp-MS has been reported [13]. Various forms of PRM have previously been developed by the proteomics community [14], [15]. Intelligent acquisition methods (i.e., TOMAHAQ [16], SureQuant [17] or GoDig [18]) were developed to facilitate the application of targeted proteomics to functional signaling pathways. However, these techniques do not provide the global proteome which is especially relevant in scp-MS applications. Due to the heterogeneous nature of single cells, the global proteome provides a mean to identify cell populations and control for technical artefacts [10], [19]. Recent developments such as Hybrid-DIA have addressed these issues by combining DIA with PRM acquisitions [20]. However, the required long ion injection times (IITs), combined with fast sample separation on short gradients typically used for scp-MS [21], call for specific scp-MS tailored hybrid data acquisition methods.

Here we present informed-DIA (iDIA) – an scp-MS specific combination of targeted acquisition based on wide window (ww)PRM, while concomitantly providing global proteome coverage based on DIA. We developed iDIA to be compatible with long IITs and fast sample separation, while being readily applicable without the need of an instrument-specific Application Programming Interface (API) or any manual post-acquisition data processing prior to raw file database searches. We observed a significant reduction in the limit of quantification (LOQ) through targeted acquisitions in scp-MS. Furthermore, we demonstrate that iDIA retains the global proteome and recapitulates the cellular hierarchy of the hematopoietic stem and progenitor compartment. Finally, we could quantify key transcription factors during cellular differentiation of hematopoietic stem and progenitor cells through wwPRM integrated into iDIA. With that, we obtained a first scp-MS protein level transcription factor focused dataset of the hematopoietic stem and progenitor compartment.

Results

Increasing sensitivity in low-input proteomics across MS-instrumentation

We assessed the application of parallel reaction monitoring (PRM) across two instrumental setups to explore targeted MS2 acquisitions as a means to increase sensitivity in low-input proteomics. Sensitivity of PRM and DIA acquisitions at various IITs were measured through dilution curves of synthetic peptides in a stable proteome (≤250 pg). Based on the quantitative linear range, we could determine the limit of quantification (LOQ) of the synthetic peptides. We utilized our scp-MS optimized DIA acquisition methods as a baseline to explore whether targeted MS2 scans could extend the LOQ in low-input proteomics. To evaluate the broad applicability of the results obtained we utilized two independent synthetic peptide pools that we acquired on a Thermo Scientific™ Orbitrap Eclipse™ Tribrid™ MS, as well as a Thermo Scientific Orbitrap™ Astral™ MS and a Thermo Scientific Orbitrap™ Astral™ Zoom MS (**Figure 1A**) Experiments on the Orbitrap Eclipse MS were performed with 10 synthetic peptides and their equivalent stable-isotopically labeled (SIL) versions, diluted in a stable 250 pg HeLa digest. On the Orbitrap Astral Zoom MS, 61 synthetic peptides were diluted in a 100 pg Yeast and *E.coli* digest. The synthetic peptides were diluted in 16 steps through the respective proteome matrix, not exceeding it. (**Figure 1B**) The number of synthetic peptides was based

on the IIT required for DIA scp-MS on the respective instruments. While DIA MS2 scans on the Orbitrap Eclipse MS were performed at maximal (max) IIT of 246 ms, Astral MS2 scans were performed at 40 ms max IIT. We could observe that PRM acquisitions on the Orbitrap Eclipse MS reach overall lower median LOQs at 118 ms (1.3-fold lower) as well as 246 ms (2.5-fold lower) compared to DIA acquisitions (**Figure 1C**). Furthermore, DIA quantification was performed on the MS1 level on both instruments due to the higher number of points per peak that could be reached for quantification. PRM acquisitions of different max IITs were kept at a stable points-per-peak to ensure consistent accuracy and precision, with results only impacted by max IIT (**Figure 1D**). We could confirm these findings on the Orbitrap Astral MS, where we also reached significantly lower LOQs for PRM acquisitions compared to DIA acquisitions when quantifying 61 synthetic peptides. We ensured that the quantification using Orbitrap and Astral mass analyzers remained comparable by showcasing no significant difference between DIA MS1 and DIA MS2-based quantification (**Figure 1E**). Two-fold lower median LOQ was reached with 40 ms max IIT and four-fold lower LOQ with 80 ms max IIT (**Figure 1 F, G**). On both instruments, we could observe an improvement in overall LOQ corresponding to longer IITs. Overall, targeted acquisition methods decreased the median LOQ of peptides in low-input proteomics across instruments.

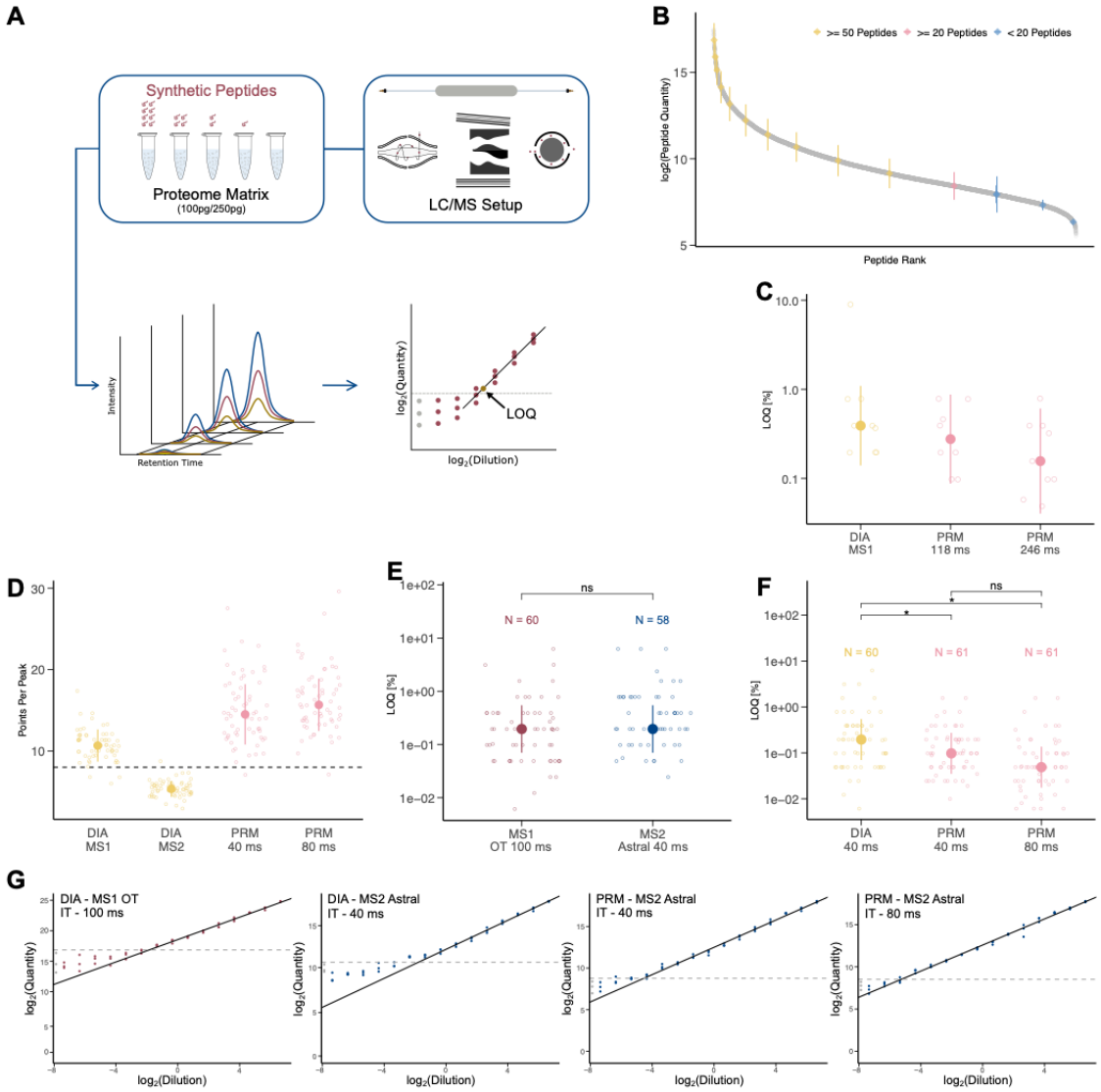

Figure 1. Assessing the sensitivity of parallel reaction monitoring (PRM) for low-input proteomics on the Orbitrap Eclipse MS and Orbitrap Astral Zoom MS. (**A**) Experimental setup to compare DIA and PRM acquisitions (**B, D-G**) Quantitative comparison of PRM and DIA acquisitions on an Orbitrap Astral Zoom MS using a dilution curve of 61 synthetic peptides over 16 points in a 100 pg yeast and *e. coli* digest including blank, Median and MAD shown (**B**) Rank plot of mean peptide quantity of each peptide in the 100 pg yeast and E.coli digest with >66 % completeness across injections. Median and MAD of synthetic peptides identified at each dilution point. (**C**) LOQ of 10 synthetic light peptides quantified by ratio to SIL peptides on the Orbitrap Eclipse MS. Peptides were quantified via our gold standard DIA method based on MS1 peak area at 246 ms max IIT, PRM acquisition at 118 ms and 246 ms max IIT. Median and MAD are shown for each condition. (**D**) Points-per-peak of 61 peptides between integration boundaries in Skyline. PRM points-per-peak were kept comparable by means of MS2 dummy scans. The dashed line indicates 8 points per peak. (**E, F**) Number of peptides for which a LOQ could be determined. Number of peptides displayed above each condition. (**E**) LOQ of 61

synthetic peptides acquired in DIA quantified both on Orbitrap MS1 (100 ms max IIT) and Astral MS2 (40 ms max IIT) level. (**F**) LOQ of 61 synthetic peptides. Peptides were quantified via our gold standard DIA method based on MS1 peak area at 100 ms max IIT on the Orbitrap mass analyzer, PRM acquisition at 40 ms and 80 ms max IIT on the Astral mass analyzer. (**G**) Example dilution curve of peptide EADDIVNWLK. Representative peptide closest to the median of all conditions. Raw peak area of top 3 y-ions displayed (3 replicates per dilution point). Peak area without synthetic peptide displayed in gray. Mean + 2*sd around peak area without synthetic peptide shown as dashed line. T-test corrected by Benjamini & Hochberg

Wide window PRM approach increases multiplexing capability in low-input proteomics

To improve reproducible quantification of peptides, the addition of SIL peptides in targeted MS acquisitions is common practice. SIL peptides can be used control for LC/MS and sample matrix-related variations during acquisition. These features make them a valuable tool in scp-MS to address sensitivity losses and sample injection across runs. We evaluated the necessity of SIL peptides for quantification in low-input proteomics. To avoid overlap with our mammalian samples in this study, we selected 10 peptides based on the *Arabidopsis thaliana* proteome and evaluated their quantitative performance, both as label-free and based on the ratio to a SIL peptide (**Supplementary Figure 1 A and B**). Nine out of 10 peptides could be fitted with a linear standard curve when using a spiked-in SIL peptide for normalization. By comparison, only five out of 10 peptides were quantitative when applying label-free quantification without such spike-ins.

However, the acquisition of both heavy and light peptides with individual PRM scans leads to a doubling of the required IIT. For example, a peptide with a base peak width of 5 seconds that is covered with 10 points per peak at an MS2 IIT of 80 ms on the Orbitrap Astral MS can only accommodate three co-eluting precursors when acquiring both SIL- and endogenous precursors. Therefore, we explored the application of wide window (ww)PRM in low-input proteomics. wwPRM acquires both SIL- and endogenous precursors within the same isolation window with optimized FAIMS CV and collision energy (**Figure 2A**). Optimized FAIMS CV and collision energy lead to an increased MS2 peak area compared to standard DIA settings (**Supplementary Figure 2 E-H**). The widening of the isolation window did not significantly impact the overall LOQ of 61 peptides on the Orbitrap Astral MS (**Figure**

2B). We could also observe similar LOQs between wwPRM and PRM on the Orbitrap Eclipse MS while doubling the possible IIT per target to 504 ms (**Supplementary Figure 2A**). The peptide level coefficient of variation (CV) was reduced for wwPRM acquisitions with similar or longer max IIT compared to DIA acquisitions over the dilution curve (**Supplementary Figure 2 B**). We concluded that SIL peptides allow for robust quantification in low-input proteomics. Furthermore, wwPRM can be applied in low-load proteomics without significant effects on the LOQ.

iDIA – combining high sensitivity wwPRM acquisitions with global DIA acquisition for single cell proteomics

The above demonstrated sensitivity gains of PRM and wwPRM scans come with the trade-off of not identifying a global proteome. This is a strong disadvantage for scp-MS, where samples cannot be reinjected, and where the total global proteome abundance is frequently used to ensure that a single cell sample was injected, to identify and normalize cell size, and to integrate heterogeneous cell populations. Therefore, we introduce informed-DIA – *iDIA*, a platform-independent combination of DIA and wwPRM specifically tailored towards single-cell proteomics.

In iDIA, targeted scans are not added to the DIA acquisition method as previously shown by other methods. Due to long IITs and short chromatographic base peak width commonly deployed in scp-MS, iDIA instead replaces DIA windows with wwPRM scans (**Figure 2C**). To retain quantitative accuracy for precursors identified in DIA scans, MS1 windows are kept at a constant distance, and quantification is performed on MS1 level. The number of DIA windows that are replaced depends on the number of points-per-peak that the user aims for and can be fully tailored to be experiment-specific. To replace DIA windows most efficiently, the acquisition method takes the number of precursors identified in each DIA window into account. At any given time, the DIA windows with the least number of precursors are replaced, while retaining regular window spacing. iDIA is set up directly in the method editor and is based on a targeted mass list table. The method can be run directly from the standard method editor without any additional requirements. The iDIA Generator builds the targeted mass list tables based on a DIA method, a scheduled PRM method of SIL and/or endogenous peptides, and DIA search results of the sample of

interest (**Figure 2F**). To ensure broad applicability, we next evaluated the compatibility of iDIA-generated raw files with commonly used DIA search engines. Single HEK-293T cells and Pierce HeLa digest was acquired with standard DIA and iDIA containing 5 or 9 scheduled wwPRMs over the retention time of 0.5 or 0.7 min each on both the Orbitrap Astral Zoom MS and the Orbitrap Eclipse MS. The resulting raw files were searched with Spectronaut 19.9 and DIANN 2.1 [22] (**Figure 2D, E**). On the Orbitrap Astral Zoom MS, 82.7 % (DIANN) and 84.7 % (SN) of the protein IDs were retained by iDIA, while 74 % and 72.3 % of the precursors remained. On the Orbitrap Eclipse MS, 70 % (DIANN) and 63.6 % (SN) of protein IDs were maintained (Precursors 58.4 % and 46.9 %) (**Supplementary Figure 2C, D**), highlighting an acceptable proteome loss associated with our hybrid method.

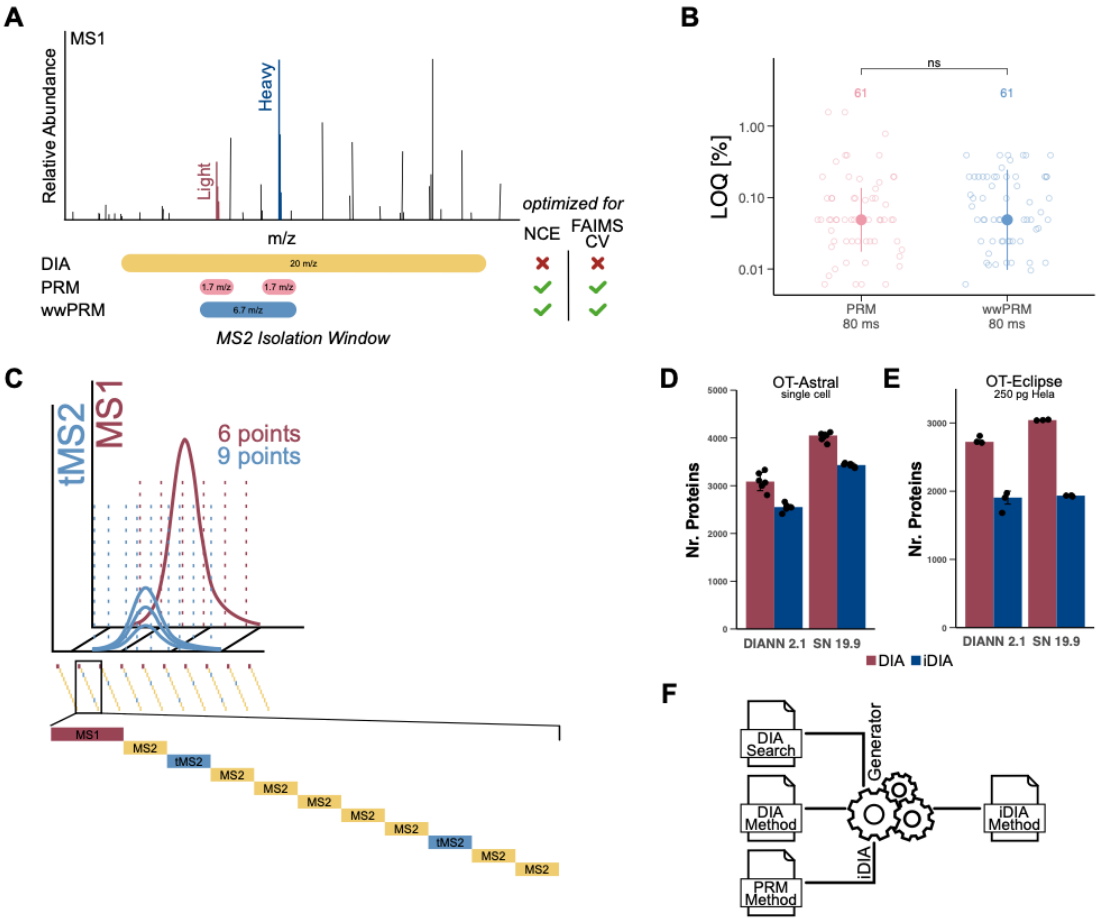

Figure 2 wide-window-(ww)PRM and informed DIA (iDIA) acquisition method. (**A**) Theoretical MS1 spectrum containing a peptide that is present both as endogenous (light) and synthetic (heavy)

peptide. MS2 isolation windows of DIA, PRM and wwPRM acquisitions displayed. (**B**) Quantitative comparison of PRM and wwPRM acquisitions on an Orbitrap Astral Zoom MS using a dilution curve of 61 synthetic peptides over 16 points in a 100 pg yeast and e. coli digest, Median and MAD shown. T-test corrected by Benjamini & Hochberg (**C**) iDIA acquisition approach. DIA acquisitions (MS2) are performed in combination with wwPRM scans (tMS2). wwPRM scans replace DIA scans to maximize points-per-peak for the wwPRM scans. DIA-quantification is performed at the MS1 level to maintain enough points-per-peak. (**D, E**) Comparison of standard DIA acquisition (Red) and iDIA acquisition (Blue) approach. Number of proteins identified in iDIA acquisitions by DIANN 2.1 and SN 19.9 (**D**) Single HEK-293T cells acquired on an Orbitrap Astral Zoom MS, 9 theoretical peptides are acquired with wwPRM replacing two out of 30 DIA windows per DIA cycle. (**E**) 250 pg HeLa digest acquired on an Orbitrap Eclipse MS, 5 theoretical peptides are acquired with wwPRM replacing 6 out of 6 DIA windows per DIA cycle. (**F**) iDIA method generation workflow.

Evaluation of iDIA acquisitions in 50 pg HeLa Digest

We assessed the applicability of iDIA based on three DIA methods in a 50 pg HeLa digest matrix spiked with 34 SIL peptides (**Table 1**, **Table 2**). We first evaluated the impact of the number of wwPRM targets acquired with iDIA. We built three iDIA methods containing 10, 20, and 34 peptides that were acquired over 30-second scheduled wwPRM scans (**Figure 3A**). We could observe an increased loss of peptides and proteins identified in the global proteome compared to standard DIA for all three DIA methods with different window widths and IITs (**Figure 3B, C**). A maximum of 24.2 % of the global proteome was lost when acquiring 34 peptides in wwPRM during iDIA acquisition at 80 ms max IIT.

We demonstrated above that longer IITs decrease the LOQ in PRM and wwPRM. Therefore, we explored iDIA methods that allow for longer wwPRM IIT compared to DIA IIT (**Figure 3D**). DIA windows were either replaced (same IIT of wwPRM and DIA MS2), the wwPRM scan window was extended to 100 ms (longer IIT of wwPRM than DIA MS2) or the wwPRM scan replaced two consecutive DIA windows (wwPRM scans have twice the IIT of DIA scans in MS2). Replacing two consecutive DIA windows with one wwPRM scan reduced the number of identified peptides on average by 21.2 % compared to standard iDIA. The extension of the wwPRM IIT to 100 ms further decreased the peptide coverage by 4.9 %. The lower the number of DIA windows remaining in the DIA methods, the more peptides were lost, highlighting the necessary balance between DIA isolation windows and DIA IIT (**Figure 3E, F**). The number of MS1 points-per-peak was kept stable in all iDIA and

DIA methods, ensuring stable MS1-based quantification (**Supplementary Figure 3A**).

We determined that the iDIA method for 34 wwPRM targets acquired at 100 ms based on a 60 ms DIA IIT with 20 DIA windows at 20 m/z width provided an optimal balance between wwPRM sensitivity and global proteome coverage. We compared the quantitative performance of the DIA acquisition during iDIA to its equivalent standard DIA acquisition. We observed a Pearson correlation of 0.92 at the protein level and 0.9 at the peptide level (**Figure 3G, H**). The correlation was slightly lower compared to Pearson correlations between DIA (0.96) or iDIA (0.94) acquisitions (**Supplementary Figure 3B, C**).

Next, we addressed the number of DIA windows that are replaced per wwPRM scan. This measure controls the number of points-per-peak for each peptide quantified by wwPRM. We compared the replacement of three and two out of 20 DIA windows per DIA cycle for each of 34 wwPRM-Peptides. We could observe a decrease of peptide IDs by 13.1 % from a mean of 5657 to 4914 identified peptides (**Figure 3 I**). Meanwhile, the median number of points per peak at wwPRM level increased from 8 to 11 with a higher number of DIA windows replaced (**Figure 3J**). These increases in wwPRM windows lead to a decrease (not significant) in median LOQ (**Figure 3 K**).

Here we demonstrated that iDIA allows for reproducible and sensitive quantification of target peptides in wwPRM while maintaining global proteome coverage. iDIA can be balanced between DIA focus and wwPRM-focused quantification based on the number of DIA windows replaced, the DIA acquisition chosen, and the number of wwPRM peptides quantified. A DIA-focused quantification of 10 Peptides in wwPRM can maintain 95 % peptide ID, while a wwPRM-optimized iDIA method of 34 targets remains 72.9 % peptide ID coverage.

Table 1. DIA MS2 acquisition settings compared in Figure 3.

Max. IIT [ms]	Nr. MS2 DIA windows	DIA window width [m/z]	Loop control [N]
40	30	13.4	16
60	20	20	10
80	16	26.6	8

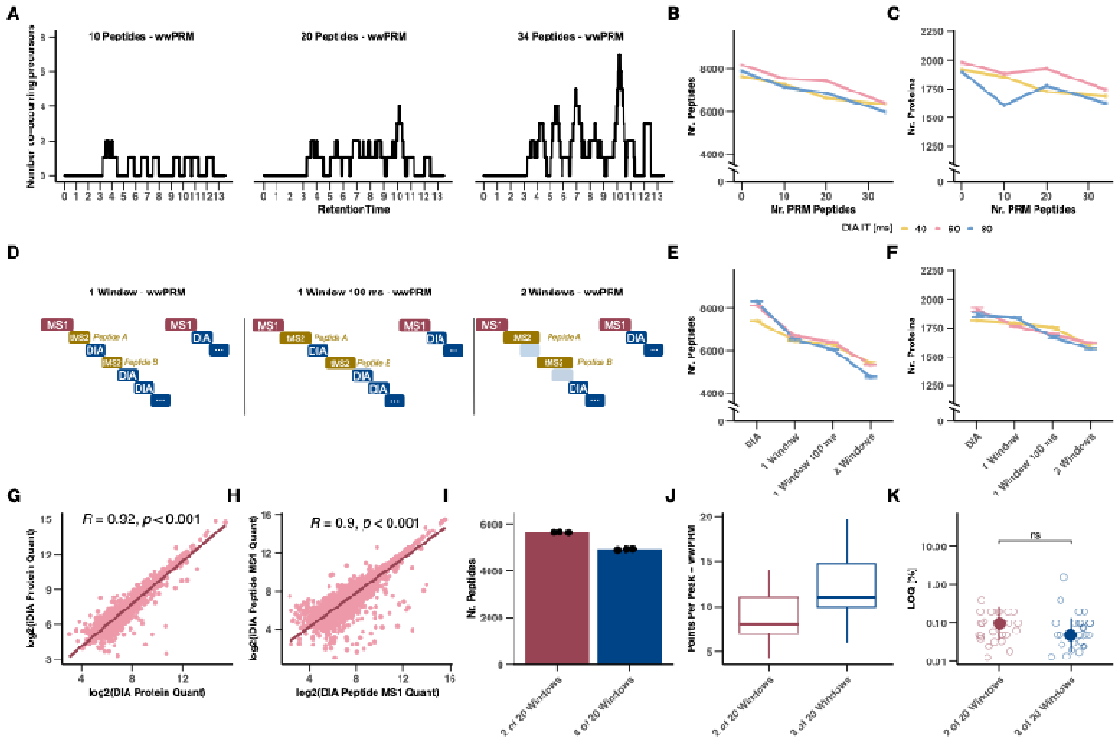

Figure 3 iDIA performance evaluation in 50 pg HeLa digest (**A-K**) 34 SIL peptides were spiked into 50 pg HeLa digest and acquired with iDIA methods based on the three DIA methods displayed in Table 1. (**A**) Number of co-occurring precursors that are acquired in wwPRM scans during iDIA method. (**B, C**) Number of peptides and proteins identified in triplicate acquisition of iDIA method, quantifying 10, 20, or 34 peptides with wwPRM scans compared to DIA. (**D**) Schematic of iDIA acquisition options. Replacement of a DIA window with a wwPRM scan, replacement and extension of max IIT of a DIA window with a wwPRM scan, or replacement of two DIA windows by one wwPRM scan. (**E, F**) Number of peptides and proteins identified in triplicate acquisition of iDIA methods shown in D. (**G, H**) Pearson Correlation of peptide and protein level quantification of peptides identified in DIA search during iDIA acquisition. Correlation between example DIA acquisition and iDIA acquisition with a 60 ms max IIT and 20-window DIA method. (**I-K**) iDIA acquisition with 2 or 3 DIA windows replaced per DIA cycle. (**I**) Number of peptides identified by SN 19.9 (**J**) Points-per-peak of 34 peptides acquired in wwPRM scans during iDIA acquisition. (**K**) LOQ of 34 SIL peptides in wwPRM.

Table 2. Transcription factor peptide panel

Protein Gene	Protein Name	Protein Accession	Peptide Sequence
Cebpa	CEBPA_MOUSE	P53566	LEPLYER
			GLAGAHPDLR
			VLELTSDNDR
Cebpe	CEBPE_MOUSE	Q6PZD9	GGQQPLEFSGGR
Erg	ERG_MOUSE	P81270	VIVPADPTLWSTDHVR
Fli1	FLI1_MOUSE	P26323	VIVPADPTLWTQEHVR
			ATSAYNTEVLLSHLSYLR
			EDPSYDSVR
Gata1	GATA1_MOUSE	P17679	SNNTFLDTLK
			ECVNCGATATPLWR
Gata2	GATA2_MOUSE	O09100	EVAPEQPR
			ECVNCGATATPLWR
Gfi1	GFI1_MOUSE	P70338	LLLGGGSYK
Gfi1b	GFI1B_MOUSE	O70237	AQGDELVWPPAVIPVAK
Hoxa9	HXA9_MOUSE	P09631	YAPGTLGQPPR
Ikzf1	IKZF1_MOUSE	Q03267	SGLIYLTNHINPHAR
			AASENSQDAFR
			VVSTSGEQLK
Ikzf2	IKZF2_MOUSE	P81183	VQDLQGEGGIR
			VFNGEGEQIR
Irf8	IRF8_MOUSE	P23611	SPDFEEVTDR
			SQLDISEPYK
			ELQQFYATQSR
Klf1	KLF1_MOUSE	P46099	AQPSYSDSR
			AGSVGGFFPR
Lyl1	LYL1_MOUSE	P27792	PSLLQLTALGR
Mecom	MECOM_MOUSE	P14404	FGPYMGEQR
Runx1	RUNX1_MOUSE	Q03347	FTPPSTALSPGK
			LEEAVWRPY
Spi1	SPI1_MOUSE	P17433	GTFQFSSK
			LTYQFSGEVLGR
Tal1	TAL1_MOUSE	P22091	AAPAEPPVIELGAR
			QQNVNGAFAELR
			YINFLAK
Tcf3	TFE2_MOUSE	P15806	SSSQYYPSFPSNPR

Quantifying transcriptional regulators in single cKIT+ murine bone marrow cells in hematopoiesis

The hematopoietic stem and progenitor cell (HSPC) hierarchy constitutes a continuous differentiation system where lineage cell fate decisions are (in part) regulated by the actions of transcription factors. We hypothesized that the gained sensitivity through iDIA would allow for the study of transcription factor regulation in single murine bone marrow (BM) cells with scp-MS. To this end, we isolated and flow-sorted cKIT+ BM HSPCs using fluorescence-activated cell sorting (FACS) (**Supplementary Figure 4**). cKIT+ cells contain hematopoietic stem cells (HSCs), which differentiate into multipotent progenitors (MPP) and further into oligopotent common myeloid (CMP) and lymphoid progenitors (CLP), establishing the myeloid, lymphoid, and megakaryocyte/erythroid lineages that characterize the blood hierarchy.

We developed a transcription factor (TF) panel of 34 peptides covering 19 TFs based on previously acquired 500-cell data and literature (**Table 2**) [23]. We established a PRM method based on the SIL peptides of the TF panel. Next, we combined the PRM and DIA method into one iDIA method, covering all 34 peptides with 100 ms wwPRM scans at a median 11 points per peak, replacing three DIA windows per wwPRM peptide in each cycle, as shown in Figure 3. We determined the LOQ for each heavy peptide and spiked the SIL peptides above LOQ to each digested single cell. On average, we could quantify 1092 proteins per cell using standard DIA and 817 proteins with the iDIA method (n = 12) (**Supplementary Figure 5A, B**). The identified number of proteins scaled well with previously published work of primary human bone marrow cells and the relatively small size of these murine cells [4]. To assess the applicability of iDIA in the context of combined TF detection and scp-MS proteome readout in HSPCs, we sorted 0, 1, 5 and 10 cKIT+ cells and acquired them with iDIA. Due to the heterogeneous nature of the cell populations, the quantified TFs are not expected to scale linearly. However, these higher cell number sorts might contain cell populations with low frequencies such as HSCs. We could demonstrate that the overall proteome coverage scaled with the number of cells sorted and that we had low background noise in the 0-cell wells (**Figure 4B, Supplementary Figure 5C**). The 0-cell wells were used to establish a signal baseline for our wwPRM quantification of TFs. 30 TF-peptides displayed a signal increase above baseline and scaled in part with the number of cells (**Figure**

4C, D, E). To ensure robust quantification, we calculated the CV of the raw peak area of each SIL peptide across 0 to 10 cell samples using five fragment ions for quantification. Across and within each cell number, we obtained median CVs below 4.7 %, highlighting the robustness of the SIL peptide spike-in to single cells. Furthermore, we could confirm that the spike-in was robust across different cell numbers. This allowed us to conclude that the variation in cell size during scp-MS was not affecting the quantification (**Figure 4F**).

After quality control, 580 single cKIT+ cells were acquired with iDIA (**Supplementary Figure 6**). We identified the global proteome using DIA-NN 2.1, processed the wwPRM data through Skyline [24] , and combined the proteomics data with the index data for 11 FACS markers. The peak areas of TF peptides with a peak area below two standard deviations around the mean of the 0-cell wells were set to zero.

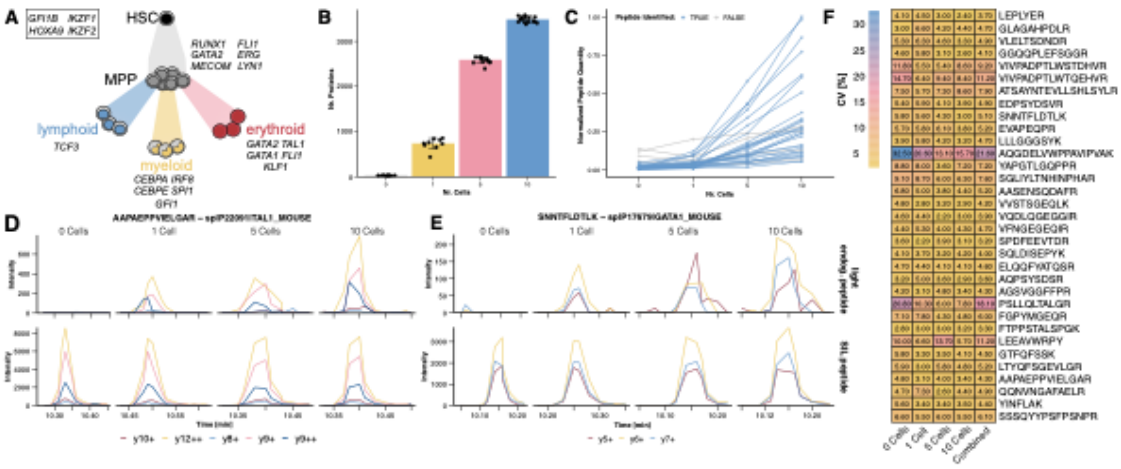

Figure 4 Quantification of Transcriptional Regulators in cKIT+ murine bone marrow cells (**A**) cKIT+ cell population with respective TFs in iDIA panel (**B-E**) 0, 1, 5 and 10 cKIT+ cells acquired in iDIA (**B**) Identified number of proteins median and mad shown. (**C**) Median ratio between endogenous and SIL peptides of TF panel (**D-E**) Example XICs for SIL and endogenous peptides. 1, 5 and 10 cells show the max. light peak area, 0 cells show the light signal closest to median peak area. (**F**) CV of SIL raw peak area of the top 5 fragments for each peptide.

We used the simultaneously identified global proteome data to project the cKIT+ cells in a low-dimensional UMAP embedding. By overlaying the FACS markers onto the embedding, we could confirm and define two differentiation trajectories: the myeloid branch (FcgR+CD34+Sca1-), and the erythroid branch (Sca1-, CD150+, CD105+, FcgR-, CD34-) (**Figure 5A**). Colocalization of the FACS markers could be observed, suggesting the global proteome information obtained by iDIA captured

biologically meaningful information in primary stem and progenitor cells (**Supplementary Figure 7**).

Next, we visualized our wwPRM-quantified TFs onto the embedding to determine if the targeted TF measurements aligned with the expected populations determined by their cell surface markers. Expression patterns could be observed for 10 out of 19 TFs, while the remaining require further investigation to determine how their expression might be modeled with our data. We observed a clear increase in TAL1 and GATA1 abundance in the erythroid branch, in accordance with previous reports from bulk proteomics by Gillespie *et al.* and Üresin *et al.* [9], [23]. Furthermore, SPI1 and CEBPA were only quantified in CD34+ and FcgR+ myeloid cells and not present at detectable levels in the remaining cell populations (**Figure 5B**) [23]. This highlighted that the three modalities of global proteome, FACS markers, and targeted wwPRM-derived TF readouts concluded the same findings. To further strengthen the confidence in the quantitative precision of the TF panel, we relied, where possible, on multiple peptides for quantification. Two independent peptides representing Tal1 and CEBPA displayed the same correlation for increased expression for erythroid lineage correlated with the CD105 or myeloid lineage correlated with FcgR expression (**Figure 5C, D**). We could not observe a direct correlation with cell size (**Supplementary Figure 6D**). Together, this underlies that by leveraging iDIA we could capture cell state-specific TF abundances, which were previously inaccessible.

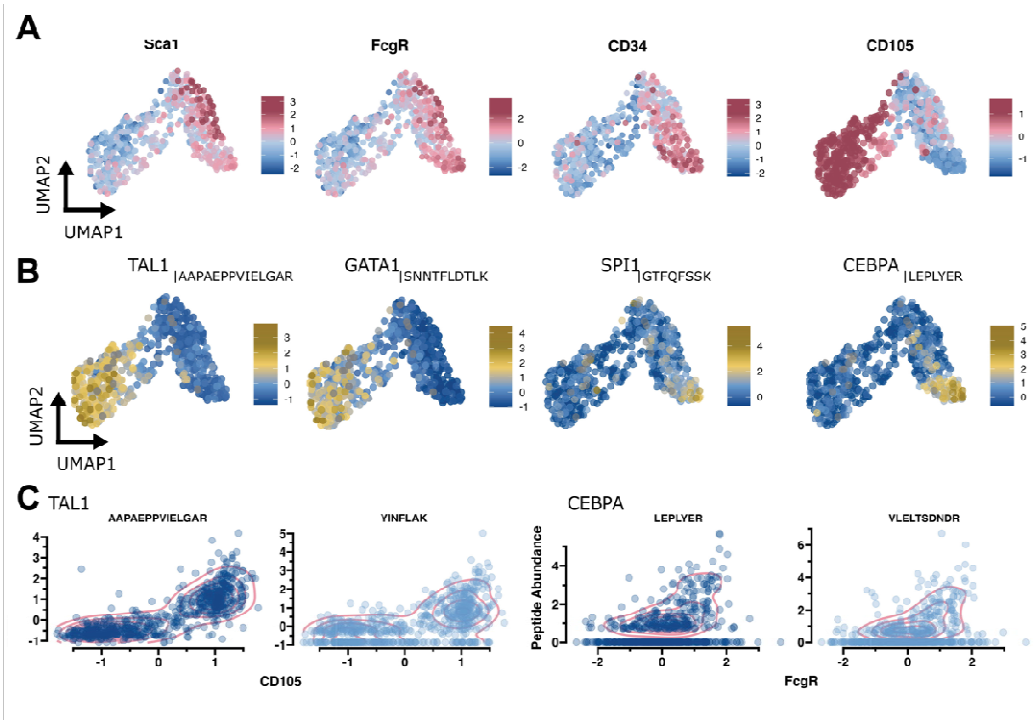

Figure 5 Integration of TF quantification with global cKIT+ cell proteomes (**A, B**) UMAP embedding based on global cell proteome (**A**) overlayed with FACS surface markers (**B**) overlayed with peptide-level TF quantification based on wwPRM (**C, D**) correlation of lineage-specific TF peptides with lineage-specific FACS cell surface markers. FACS markers and TF expression were z-scored for ease of visualization.

Discussion

Here we present iDIA, a new data acquisition method tailored towards low-input and single-cell proteomics. iDIA allows quantification of targets of interest with significantly higher sensitivity and selectivity. The method has been shown to be applicable across multiple MS instruments and does not require specialized software to be executed. iDIA reduces the number of DIA scans to accommodate targeted wwPRM acquisitions and demonstrated higher sensitivity and reduced LOQ when quantifying targets of interest. Nevertheless, iDIA only results in a minor hit proteome depth, and delivers biologically informative global proteomes. Previously published combined targeted and global acquisition methods led to prolonged cycle times and relied on the use of API and further post-acquisition data processing steps. We build upon these methods with the specific purpose for scp-MS application, by keeping stable cycle times throughout the acquisition method. Consequently, the method

becomes compatible with narrow chromatographic peak widths and the prolonged IIT necessary for scp-MS experiments.

Due to the very limited input material in scp-MS the reproducible quantification of a panel of low-abundant transcription factors has been challenging so far. By utilizing targeted MS2 scans with SIL peptides, iDIA gained the selectivity and specificity to quantify transcription factors at single-cell resolution in primary murine bone marrow cells. To the best of our knowledge, this has never been achieved before. The global proteome of each single cell contained enough information to recapitulate the cellular hierarchy of the hematopoietic stem and progenitor compartment. We could confirm this through integration with the index FACS data. By further integrating the quantified TFs onto the global proteome, a peptide-based single-cell TF map of the hematopoietic stem and progenitor compartment could be constructed. We showcased unique expression patterns for both myeloid and erythroid branches of the progenitor compartment. Furthermore, we could confirm the quantification of TAL1 and CEBPA by multiple peptides.

Through the simultaneous measurement of global proteome and targeted TFs, we were able to quantify very low-abundant TFs in single hematopoietic stem and progenitor cells of the murine bone marrow**.** iDIA allowed the seamless integration of both modalities to gain novel insights into the regulation of hematopoiesis. With its ease of implementation and strong performance, we expect a widespread adoption of iDIA across multiple life science domains, where such specificity is essential for biological insights of e.g post-translational modifications.

Author Contributions

J.W., B.T.P., and E.M.S. designed the study. J.W. and S.S. performed the experiments. J.W. and V.P. performed data analysis, with input from B.F. J.W. designed the methods and evaluated the data, with input from V.P., S.S., T.A., B.F., J.o.d.B, E.D., B.T.P., and E.M.S. The manuscript was drafted and revised by J.W., V.P., B.T.P. and E.M.S., and has been read and approved by all authors. B.T.P. and E.M.S. supervised the work.

Acknowledgements

This work was funded by the following grants to E.M.S.: 1) reference number NNF21OC0071016 from the Novo Nordisk Foundation; 2) case no. 2067-00053B

from the Independent Research Fund Denmark., 3) Lundbeck Foundation (R413-2022-869) and 4) the DigitSTEM initiative, funded by Bioneer A/S. Work in the Porse lab was supported by grants from the Svend Andersen Foundation, the Danish Cancer Society, the Eva and Henry Frænkel Memorial Foundation, and the Independent Research Fund Denmark. This work has been performed in the context of the Danish Research Center for Precision Medicine in Blood Cancers funded by the Danish Cancer Society (R223-A13071) and Greater Copenhagen Health Science Partners.

Conflict of Interest Disclosure

The authors declare the following competing financial interest(s): The Schoof lab at the Technical University of Denmark has a sponsored research agreement with Thermo Fisher Scientific, the manufacturer of the instrumentation used in this research. However, analytical techniques were selected and performed independently of Thermo Fisher Scientific. T.N.A., J.o.d.B., E.D. are employees of Thermo Fisher Scientific, the manufacturer of the instrumentation used in this research.

Reference

[1] T. M. Peters-Clarke, J. J. Coon, and N. M. Riley, “Instrumentation at the leading edge of proteomics”.

[2] J. A. Bubis *et al.*, “Challenging the Astral mass analyzer to quantify up to 5,300 proteins per single cell at unseen accuracy to uncover cellular heterogeneity,” *Nat. Methods*, vol. 22, no. 3, pp. 510–519, Mar. 2025, doi: 10.1038/s41592-024-02559-1.

[3] Z. Ye *et al.*, “Enhanced sensitivity and scalability with a Chip-Tip workflow enables deep single-cell proteomics,” *Nat. Methods*, vol. 22, no. 3, pp. 499–509, Mar. 2025, doi: 10.1038/s41592-024-02558-2.

[4] V. Petrosius *et al.*, “Quantitative Label-Free Single-Cell Proteomics on the Orbitrap Astral MS,” *Mol. Cell. Proteomics*, vol. 0, no. 0, May 2025, doi: 10.1016/j.mcpro.2025.100982.

[5] J. Derks *et al.*, “Increasing the throughput of sensitive proteomics by plexDIA,” *bioRxiv*, p. 2021.11.03.467007, Mar. 2022, doi: 10.1101/2021.11.03.467007.

[6] X. Sanchez-Avila, R. M. de Oliveira, S. Huang, C. Wang, and R. T. Kelly, “Trends in Mass Spectrometry-Based Single-Cell Proteomics,” *Anal. Chem.*, vol. 97, no. 11, pp. 5893–5907, Mar. 2025, doi: 10.1021/acs.analchem.5c00661.

[7] X. Xie *et al.*, “Multicolumn Nanoflow Liquid Chromatography with Accelerated Offline Gradient Generation for Robust and Sensitive Single-Cell Proteome Profiling,” *Anal. Chem.*, vol. 96, no. 26, pp. 10534–10542, Jul. 2024, doi: 10.1021/acs.analchem.4c00878.

[8] A. Leduc, R. G. Huffman, J. Cantlon, S. Khan, and N. Slavov, “Exploring functional protein covariation across single cells using nPOP,” *Genome Biol. 2022 231*, vol. 23, no. 1, pp. 1–31, Dec. 2022, doi: 10.1186/S13059-022-02817-5.

[9] M. A. Gillespie *et al.*, “Absolute Quantification of Transcription Factors Reveals Principles of Gene Regulation in Erythropoiesis,” *Mol. Cell*, vol. 78, no. 5, pp. 960-974.e11, Jun. 2020, doi: 10.1016/j.molcel.2020.03.031.

[10] B. Furtwängler *et al.*, “Mapping the human hematopoietic stem and progenitor cell hierarchy through integrated single-cell proteomics and transcriptomics,” Jul. 06, 2024, *bioRxiv*. doi: 10.1101/2024.07.05.602277.

[11] A. C. Peterson, J. D. Russell, D. J. Bailey, M. S. Westphall, and J. J. Coon, “Parallel Reaction Monitoring for High Resolution and High Mass Accuracy Quantitative, Targeted Proteomics *,” *Mol. Cell. Proteomics*, vol. 11, no. 11, pp. 1475–1488, Nov. 2012, doi: 10.1074/mcp.O112.020131.

[12] V. Lange, P. Picotti, B. Domon, and R. Aebersold, “Selected reaction monitoring for quantitative proteomics: a tutorial,” *Mol. Syst. Biol.*, vol. 4, no. 1, p. 222, Jan. 2008, doi: 10.1038/msb.2008.61.

[13] A. Eshghi *et al.*, “Sample Preparation Methods for Targeted Single-Cell Proteomics,” *J. Proteome Res.*, Apr. 2023, doi: 10.1021/acs.jproteome.2c00429.

[14] D. Nam *et al.*, “Wideband PRM: Highly Accurate and Sensitive Method for High-Throughput Targeted Proteomics,” *Anal. Chem.*, vol. 96, no. 25, pp. 10219–10227, Jun. 2024, doi: 10.1021/acs.analchem.4c00518.

[15] S. Gallien, A. Bourmaud, S. Y. Kim, and B. Domon, “Technical considerations for large-scale parallel reaction monitoring analysis,” *J. Proteomics*, vol. 100, pp. 147–159, Apr. 2014, doi: 10.1016/j.jprot.2013.10.029.

[16] Q. Yu *et al.*, “Sample multiplexing for targeted pathway proteomics in aging mice,” *Proc. Natl. Acad. Sci. U. S. A.*, vol. 117, no. 18, pp. 9723–9732, May 2020, doi: 10.1073/pnas.1919410117.

[17] L. E. Stopfer *et al.*, “High-Density, Targeted Monitoring of Tyrosine Phosphorylation Reveals Activated Signaling Networks in Human Tumors,” *Cancer Res.*, vol. 81, no. 9, pp. 2495–2509, May 2021, doi: 10.1158/0008-5472.CAN-20-3804.

[18] Q. Yu *et al.*, “Sample multiplexing-based targeted pathway proteomics with real-time analytics reveals the impact of genetic variation on protein expression,” *Nat. Commun.*, vol. 14, no. 1, Art. no. 1, Feb. 2023, doi: 10.1038/s41467-023-36269-7.

[19] V. Petrosius *et al.*, “Exploration of cell state heterogeneity using single-cell proteomics through sensitivity-tailored data-independent acquisition,” *Nat. Commun.*, vol. 14, no. 1, Art. no. 1, Sep. 2023, doi: 10.1038/s41467-023-41602-1.

[20] A. Martínez-Val *et al.*, “Hybrid-DIA: intelligent data acquisition integrates targeted and discovery proteomics to analyze phospho-signaling in single spheroids,” *Nat. Commun.*, vol. 14, no. 1, p. 3599, Jun. 2023, doi: 10.1038/s41467-023-39347-y.

[21] M. Matzinger, R. L. Mayer, and K. Mechtler, “Label□free single cell proteomics utilizing ultrafast LC and MS instrumentation: A valuable complementary technique to multiplexing,” *Proteomics*, vol. 23, no. 13–14, p. 2200162, Jul. 2023, doi: 10.1002/pmic.202200162.

[22] V. Demichev, C. B. Messner, S. I. Vernardis, K. S. Lilley, and M. Ralser, “DIA-NN: neural networks and interference correction enable deep proteome coverage in high throughput,” *Nat. Methods*, vol. 17, no. 1, pp. 41–44, Jan. 2020, doi: 10.1038/s41592-019-0638-x.

[23] N. Üresin, V. Petrosius, P. Aragon-Fernandez, B. Furtwängler, E. M. Schoof, and B. T. Porse, “Unraveling the proteome landscape of mouse hematopoietic stem and progenitor compartment with high sensitivity low-input proteomics,” May 05, 2024, *bioRxiv*. doi: 10.1101/2024.05.03.592307.

[24] B. MacLean *et al.*, “Skyline: An open source document editor for creating and analyzing targeted proteomics experiments,” *Bioinformatics*, vol. 26, no. 7, pp. 966–968, Feb. 2010, doi: 10.1093/bioinformatics/btq054.

Methods

Cultivation of HEK 293-F cells

Hek 293-F cells were cultured at 37 °C in Gibco™ FreeStyle™ 293 Expression Medium containing Penicillin and Streptavidin. Cells were washed three times in PBS prior to sorting.

Isolation of cKIT-Cells

One 13-week-old female C57BL/6 mice was sacrificed by cervical dislocation and leg bones (femur, tibia and iliac crest) and spine were isolated. The bones were crushed three times with 10 mL PBS+3% FBS and the suspension was filtered through a 70µm cell strainer. The filtered suspension was then centrifuged at 300g for 10 min at 4°C. To enrich for cKit+ (CD117+) cells, the resulting pellet was resuspended in 194µl PBS+3% FBS and 6µl CD117 MicroBeads (Miltenyi Biotec, 130-091-224) and incubated on ice for 30 min. Magnetic separation was carried out using an LS column (Miltenyi Biotec, 130-042-401), according to manufaturer's protocol.

FACS sorting

Following cKit enrichment, the BM cells were stained with antibodies on ice for 30 min (see **Supplementary table 1**). Following staining, the cells were washed three times with PBS to remove any residual serum by centrifugation at 300g for 10 min at 4 °C. The pellet was resuspended in PBS containing 1:1000 (v/v) 7-AAD viability dye (Invitrogen, A1310). Using a BD FACSymphony S6 cell sorter with a 100-micron nozzle set to single-cell sort mode, one cell was sorted into each well of an Eppendorf twin.tec 384 LoBind plate containing 1µl of 20% TFE, 80mM TEAB lysis buffer. Immediately after the sort, plates were briefly spun down, snap-frozen on dry ice, and stored at -70°C.

Sample Preparation

Single cells were sorted into a 384 well plate containing 1 µL of lysis buffer (80 mM Triethylammonium bicarbonate (TEAB) pH 8.5, 20% 2,2,2-Trifluoroethanol (TFE)). The plate was frozen to -80 °C. Prior to sample acquisition the plates were heated to 95 °C followed by a second freezing cycle to -80 °C. 1 µL containing 2 ng Trypsin Platinum (Promega) was added to each well and the plate was incubated at 37 °C overnight. The digestion was stopped by the addition of 1 % trifluoroacetic acid

(TFA). If SIL peptides were used in the experiment they were diluted to their final concentration in 1 % TFA and added to the single cells during the quenching of the digestion.

Bulk samples were pepared from Pierce™ Yeast Digest Standard, Pierce™ HeLa Protein Digest Standard or MassPREP E.coli digestion standard (Waters™). Standards were reconstituted in 0.1 % Formic Acid (FA) and diluted to the respective concentration in 0.1 % FA.

Peptide Standards

Peptide standards were ordere from JPT Peptide Technologies GmbH. Apon recieval peptides were resuspended in 0.1 % FA and stored at -80 °C. Peptides concentrations were adjusted to the respective sample matrix in an iterative process.

LC-MS analysis

Samples were analyzed using the Thermo Scientific Vanquish™ Neo UHPLC system in combination with the Orbitrap Astral MS and the Orbitrap Astral Zoom MS, as well as the Thermo Scientific UltiMate™ 3000 nano-LC combined with the Orbitrap Eclipse MS. All instruments were equipped with the Thermo Scientific FAIMS Pro™ interface or Thermo Scientific FAIMS Pro Duo interface in combination with the Thermo Scientific EASY-Spray™ Source.

.

Peptide separation was performed on the 50 cm µPAC Neo analytical column and the 50 cm µPAC Neo Plus analytical column combined with the µPAC Standard Trap Columns and the Thermo Scientific EASY-Spray™ Emitters.

On the Orbitrap Astral MS1 spectra were acquired with resolution of 240000, a maximum injection time of 100 ms and the automated gate control (AGC) was set to 500 %. During DIA acquisitions MS2 spectra were performed at an AGC of 500 % over the mass range of 400 m/z to 800 m/z at a HCD collision energy of 25. Maximum injection time (max IIT), DIA-window width and Loop Control were set to complete one full DIA cycle in approximately 1.2 seconds with a Loop Control 0.6 seconds at max IIT. Injections times of 40 ms, 40 ms, 60 ms and 80 ms were combined with a respective DIA-window width of 13.4 m/z, 13.7 m/z, 20 m/z, 26.6

m/z and a loop control (N) of 16, 15, 10, 8. FAIMS was operated at a compensation voltage (CV) of -48 V.

PRM MS2 scans on the Orbitrap Astral Zoom MS were performed at 1.7 m/z isolation width at 40 ms and 80 ms max IIT. wwPRM scans were performed at an isolation width of delta(Heavy Isotope Precursor Mass – Light Isotope Precursor Mass)/ precursor charge state + 1.7 m/z with an injection time of 80 ms. AGC was set to 500 %. Both FAIMS CV and HCD collision energy were operated at custom settings for the respective peptides. FAIMS CV was optimized between -30 V and -55 V and HCD was optimized between 20 and 33.

iDIA acquisitions were performed with MS1 scans as stated above. MS2 scans were operated at an AGC of 500 %. DIA windows were acquired with an HCD collision energy of 25 and a FAIMS CV of -48 V over the mass range of 400 m/z to 800 m/z. Windows and injections time were as described for the DIA methods above. wwPRM scans were acquired with custom HCD and FAIMS settings at max IIT's of 40 ms, 60 ms, 80 ms, 100 ms, 120 ms or 160 ms. The loop control was set to 0.6 seconds or N of 16, 15, 10 or 8. wwPRM scans were performed over 0.5 min for each target peptide. Acquisitions performed on the Orbitrap Astral Zoom MS were done with the Low Input Application Mode enabled.

On the Orbitrap Eclipse MS1 spectra were acquired at a FAIMS CV of -45 V at a Orbitrap resolution of 120000 and a max IIT of 246 ms. AGC was kept at 300 %. DIA MS2 scans were acquired at a resolution of 120000 or 240000 with a max IIT of 246 or 502 ms. DIA windows were acquired at 68 m/z width over the mass range of 400-800 m/z. AGC was kept at 1000 % with a collision energy of 26 and a FAIMS CV of - 45 V. PRM acquisitions were performed at an isolation window width of 1.7 m/z with custom collision energy and FAIMS CV settings. AGC was kept at 300 %. PRM scans were acquired at resolutions of 60000, 120000 and 240000 with the respective max IIT of 118 ms, 246 ms and 502 ms. wwPRM MS2 scans were operated at an AGC of 300 % with custom FAIMS CV and collision energy settings. Isolation windows were set to delta(Heavy Isotope Precursor Mass – Light Isotope Precursor Mass)/ precursor charge state + 1.7 m/z. iDIA acquisitions were performed at a MS1 resolution of 120000 with a maximum IIT of 246 ms. The AGC was kept at 300 % and FAIMS CV was set to - 45 V. MS2 scans were operated in a combination of DIA and wwPRM scans. DIA scans were performed over the mass range of 400-800 m/z with 68 m/z wide MS2 windows. Collision energy and AGC were set to -45 V and

300 % respectively. wwPRM scans were operated as described above with a custom FAIMS CV and collision energy for each peptide. wwPRM scans were operated over the time of 0.7 minutes for each target peptide with a loopcontrol of N=3.

For the 50 cm µPac Neo Plus analytical column the gradient was built at 600 nL/min or 750 nL/min starting at 1 % Solvent B with an increase to 10 % solvent be over the first 0.05 minutes. During the following 2.1 minutes Solvent B was increased to 22.5 %. The next 1.25 min Solvent B was increased to 37.5 % followed by an increase to 40% within 0.1 min. Solvent B was further increased to 90 % for the remainder of the gradient. At minute 3.5 of the gradient the flow was dropped to 200 nL/min. Samples were acquired over 12.5 min, 12.6 min and 13.5 min. The column was kept at 50 °C.

The 50 cm µPac Neo analytical column was operated at 50 °C. The column was loaded at 750 nL/min at 100 % Solvent A. After 0.2 min Solvent B was increased to 8 % followed by a linear increase to 24 % B until minute 3 at which point the flowrate was dropped to 200 nL/min. The linear gradient was raised to 48 % B at minute 8 and increased to 99 % B over the following 0.4 minutes. 99 % B was kept for 6.55 minutes followed by a drop to 1 % B until minute 17.85.

PRM development

Synthetic peptides were acquired in DIA and the identified precursors were subjected to a scheduled PRM scan. PRM scans were manually revised followed by PRM acquisitions at FAIMS CVs between -30 V and -55 V and HCDs between 20 and 33. Notably the MS1 scans were kept at stable FAIMS CV -45 V (Eclipse) and -48 V (Astral) and stable HCD. Only FAIMS CV and HCD of the MS2 scans was altered. The total MS2 peak area of each peptide was normalized to the MS1 peak area to identify the optimal FAIMS and HCD settings for each peptide. A peptide library was built from these optimized settings containing the top 15 b-and y ions >b2 and >y2. To address the quantitative performance of these PRM assays, standard curves were established of the synthetic peptides in a stable background matrix of 250 pg, 100 pg or 50 pg HeLa digest or combined Yeast and E coli digest.

Data Analysis

LOQ determination

Standard curves were established by performing a serial dilution of the synthetic peptides in a stable sample matrix as described above. Peptide standards were titrated into the respective matrix to start each standard curve at the highest protein expressed in the background proteome. Peptide standards were diluted over 14 to 16 dilution points with a sample containing the matrix as last point of the standard curve to model the background signal of each peptide.

Results were imported into Skyline-daily (version 25.0.9.97) and peptide peak integration was revised. All b, y and precursor ions that were part of the library were exported at fragment level peak area. The fragment level elution profile was compared to the library and the most intense top 3 y-fragment ions were selected for quantification. B-ions were only used for identification of the peptides and peak area integration. In case of wwPRM acquisitions the b-ions would be shared between heavy and light peptide and were therefore not considered for quantification. The top three y-ion peak areas of each heavy as well as light were summed. In case both heavy and light were used for quantification the ratio of the summed peak-area between heavy and light was taken. In case only light or only heavy peptides were quantified, the summed peak area was normalized to the total ion current (TIC) of the respective run. The CV between the replicates of each point of the standard curve were calculated and only replicates with a CV below 20 % were considered to fit the standard curve. The LOD of each peptide was identified by integrating the background matrix without peptide spike-in at the same retention time window as the background matrix spiked with synthetic peptides. The LOD was defined as Mean(sum peak area background matrix) + 2*Standard Deviation (sum peak area background matrix). To allow for a noise reduction during the fitting of the standard curve, replicates with a deviation from the expected linear ratio between dilution points were excluded if they had a delta variation larger then 25 %. The remaining dilution points were used to fit a linear model. Following assumptions were made when calculating the LOQ: If the fitted linear model contains the last dilution curve point above the LOD and no dilution curve point below the LOD has a replicate with a higher peak area than the LOD, the LOD is considered the LOQ. If this assumption is not met, the last point of the dilution curve that was used to fit the linear model is considered the LOQ.

iDIA setup

To compile an iDIA MS method, the preferred DIA window setting was exported from the Method Editor. Additionally, the established PRM target list containing the heavy or light version peptides of interest, their mass, retention time window, optimal FAIMS CV and optimal HCD was exported from the method editor. The sample of interest was acquired with the preferred DIA method and searched in Spectronaut 19. The precursor level search results were exported containing the m/z of each precursor and its peak area start and end. These three csv files were passed to the iDIA generator together with the information of the base peak width of the used chromatography, cycle time of the DIA method, DIA NCE and FAIMS CV as well as DIA-MS2 IIT and preferred PRM IIT. PRM methods were converted to wwPRM method if specified and the replacement of more than one DIA window with PRM scans could be specified. The iDIA method generation considered the number of precursors that were identified in each combination of DIA windows that were to be replaced by PRM scans and selected the combination of DIA windows that contained the least precursors while maintaining an equal time gap between the PRM acquisitions. PRM scans were converted into wwPRM scans which include both heavy and light peptide with a 0.85 m/z spacing before and after the light and heavy precursor. DIA windows were replaced with wwPRM scans at the specified retention time window in the PRM method. A csv file containing a combined DIA and wwPRM method that contains both scheduled DIA and wwPRM scans over the full chromatographic gradient.

DIA Search Settings

DIA and iDIA raw files were searched in both DIANN 2.1 and Spectronaut 1.9. Dependent on the sample matrix Carbamidomethyl (C) was set as a fixed modification. DirectDIA was used in Spectronaut with the respective FASTA file. Quantification was performed on the MS1 level with the FDR set to 0.01. If multiple conditions were searched together, each condition was set, and Method Evaluation was selected. In DIANN 2.1 a library was build based on the FASTA file using DIANN. Trypsin/P with 1 missed cleavage was selected and N-term Methionine excision enabled. Peptide length was set to 6-30 AA and precursor range was specified as in the DIA methods ranging from 400 m/z to 800 m/z. The FDR was set to 1 %.

Single Cell Data Processing

Raw files were searched initially with DIANN 2.1 as unrelated runs against the mouse swissprot proteome (version: 30.04.2025). Results were further processed in R. Rawfiles with a FWHM.RT larger then 0.085 were excluded from the analysis and the total number of proteins in each file was correlated with the FACS FSC-A. After this first round of QC, the remaining raw files were searched in DIANN using MBR. Single cell raw files and negative control raw files were imported into Skyline. Only MS2 spectra with a m/z window covering less than 7 m/z were imported. Peptides with overlapping retention time and isolation windows were further specified to be only extracted from their unique wwPRM window. Peak area integration was performed by Skyline on the stable heavy spike-in. A fragmentation level report was exported and processed as described above. The negative controls placed on each plate were used to model the background signal at the specific retention time contain heavy spike-in. All signal below two standard deviations around the mean negative control for each peptide was set to 0. Peptide signal above this negative control was considered as identified peptide.

Supplementary information

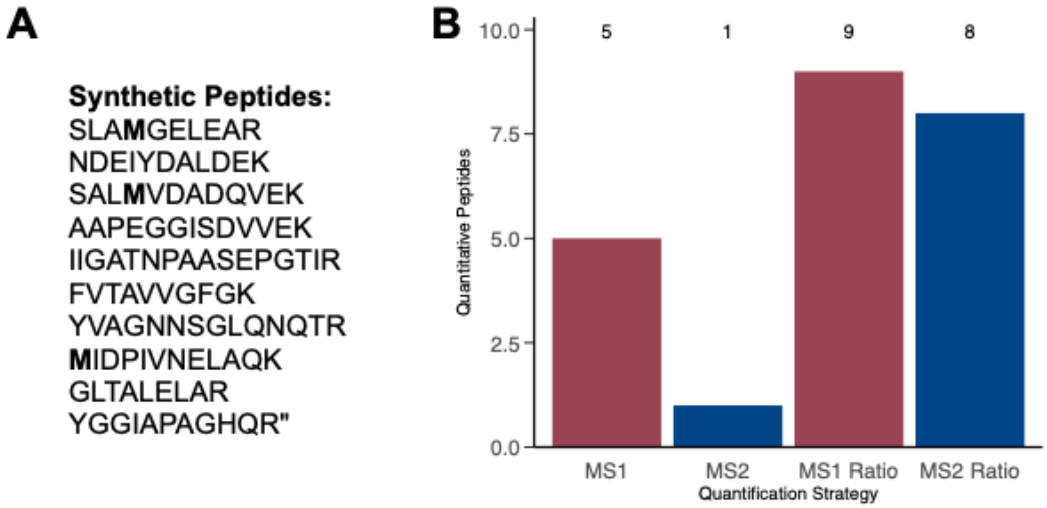

Supplementary Figure 1 Assessing stable isotope-labeled peptide standards regarding quantitative accuracy in low-input proteomics. (**A**) List of 10 peptides synthesized as heavy and light, randomly selected from the *Arabidopsis thaliana* proteome. (**B**) Number of peptides shown in A that decreased linearly in dilution curves and to which a standard curve could be fitted. Peptides quantified in DIA on an Orbitrap Eclipse MS. Heavy peptides were kept at a stable concentration throughout the dilution curve. “Ratio” refers to the quantification of light peptide in ratio to the stable spike-in of heavy peptide.

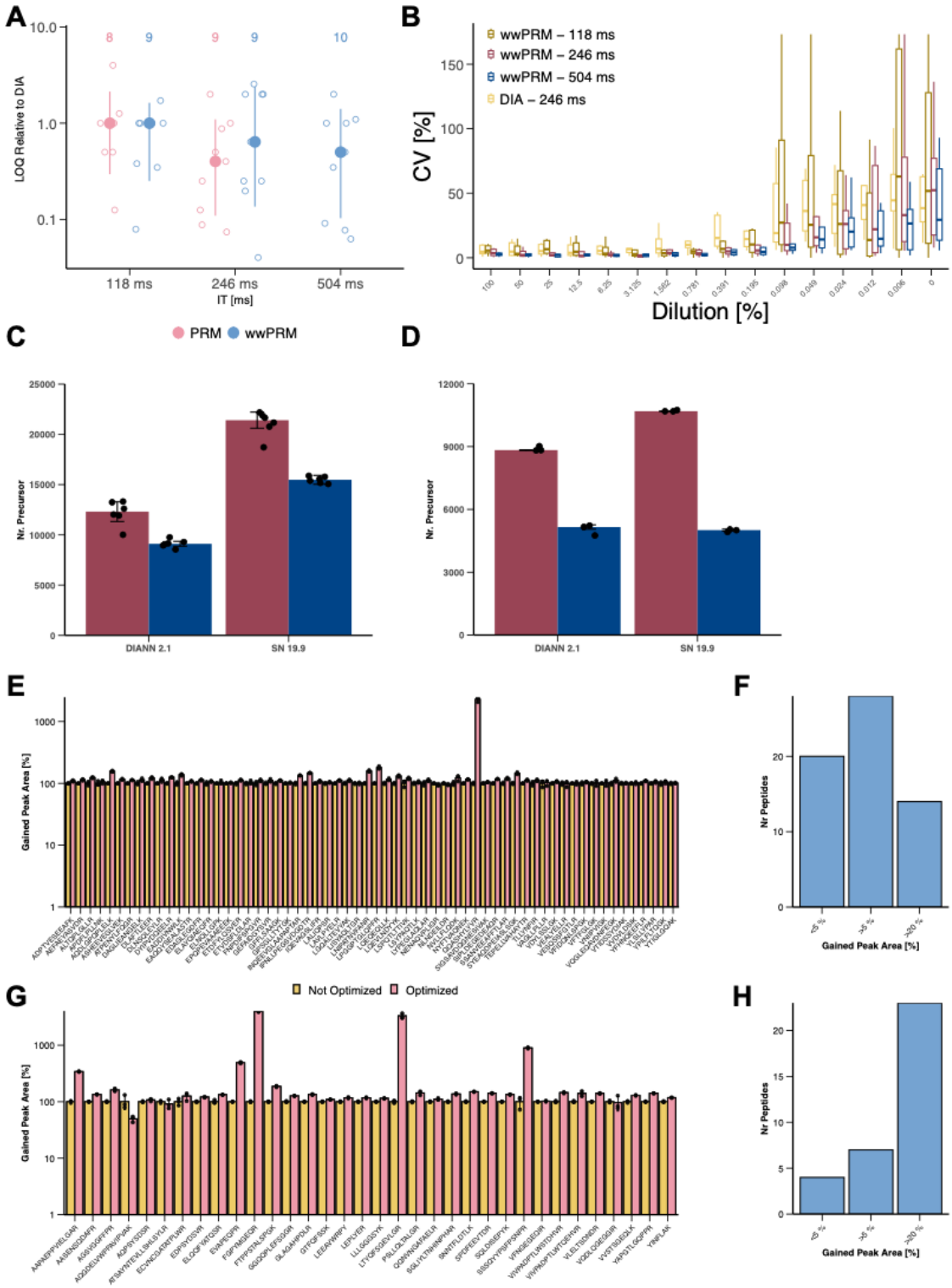

Supplementary Figure 2 wwPRM and iDIA acquisition. (**A,B**) Quantitative comparison of PRM and wwPRM acquisitions on an Orbitrap Eclipse MS using a two-fold Dilution curve of 10 synthetic peptides over 16 points in a 250 pg HeLa digest, mean and standard deviation shown. Quantification based on the ratio of light peptide to heavy standard. (**A**) LOQ of peptides acquired in PRM and

wwPRM relative to their respective LOQ in DIA. (**B**) Coefficient of variation (CV) of 10 peptides quantified in triplicate at each point of the dilution curve in DIA and wwPRM. Maximum injection times of 118 ms, 246 and 502 ms were used. (**C, D**) Comparison of standard DIA acquisition (Red) and informed (i)-DIA acquisition (Blue) approach. Number of precursors identified in iDIA acquisitions by DIANN 2.1 and SN 19.9 (**C**) Single HEK-293T cells acquired on an Orbitrap Astral Zoom MS, 9 peptides are acquired with wwPRM replacing two out of 30 DIA windows per DIA cycle. (D) 250 pg HeLa digest acquired on an Orbitrap Astral Zoom MS, 5 peptides are acquired with wwPRM replacing 6 out of 6 DIA windows per DIA cycle.(**D,E**) Percentage MS2 peak area gained with optimized NCE and FAIMS CV settings for 61 peptides compared to DIA settings. Optimized parameters used in data for Figure 1D, F, and G and Figure 2b.(**F,G**) Percentage MS2 peak area gained with optimized NCE and FAIMS CV settings for 34 peptides compared to DIA settings. Optimized parameters used in the data for Figure 3, 4, and 5.

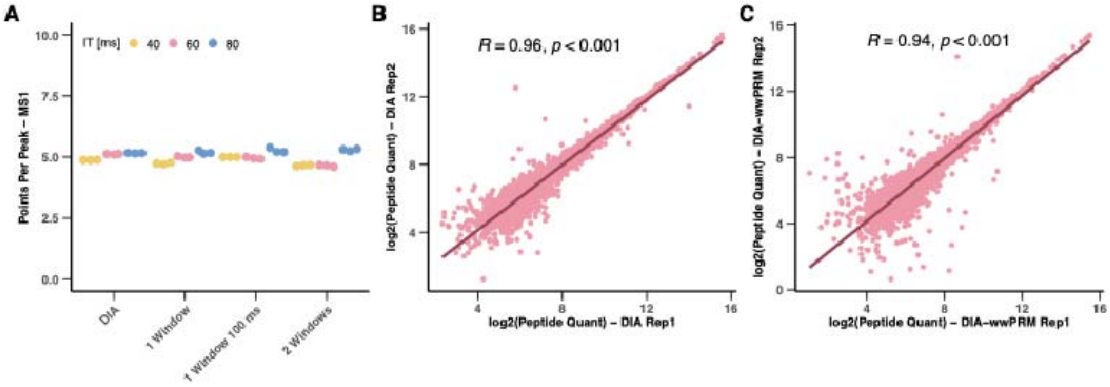

Supplementary Figure 3 iDIA performance evaluation (**A-C**) 34 synthetic heavy peptides were spiked into 50 pg HeLa digest and acquired with iDIA methods based on three DIA method displayed in Table 1. (**A**) MS1 points per peak in iDIA compared to DIA at three iDIA settings. Replacement of a DIA window with a wwPRM scan, replacement and extension of max IIT of a DIA window with a wwPRM scan or replacement of two DIA windows by one wwPRM scan. (**B**) Pearson Correlation or peptides between to representative DIA acquisitions at 60 ms max IIT with 20 windows. (**C**) Pearson Correlation or peptides between to representative iDIA acquisitions at 60 ms max IIT with 20 windows.

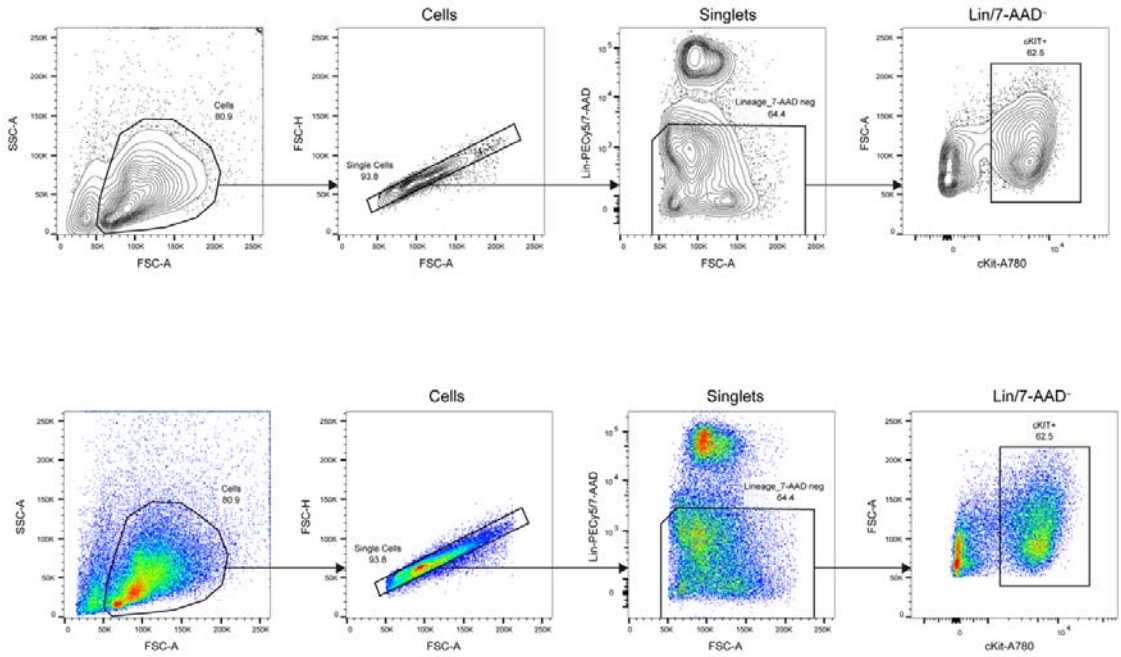

Supplementary Figure 4 FACs Isolation schema of cKIT+ positive single cells.

Supplementary Table 1 Marker panel used for cKIT+ mouse bone marrow cell-staining

Marker/Dye	Fluorophore/Channel
Mac1 (CD11b)	PE-Cy5
Gr1/Ly6 (Ly-6G/Ly-6C)	PE-Cy5
B220	PE-Cy5
CD3	PE-Cy5
CD34	FITC
Flt3 (CD135)	PE-CF594
CD150	BV650
FcgR (CD16/CD32)	A700
CD41	eF450
CD105	PE
Sca1 (Ly-6A/E)	APC
cKIT	A780
Ter119	PE-Cy7
CD71	BV510
7-AAD	PE-Cy5

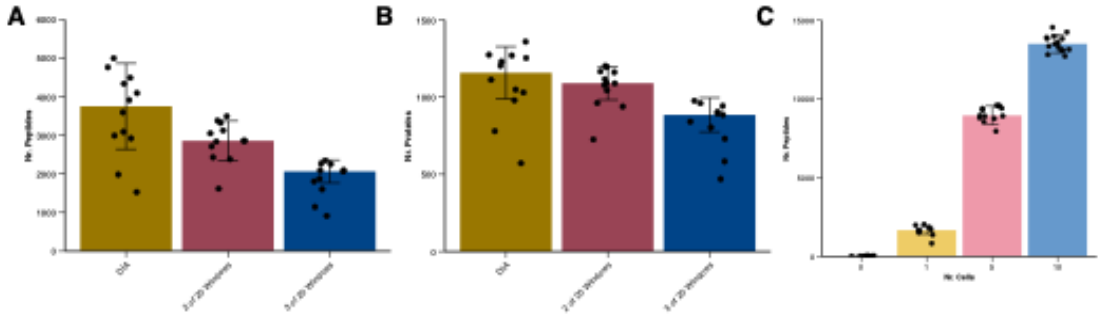

Supplementary Figure 5 cKIT+ cells acquired with iDIA (**A, B**) Number of peptides and proteins identified from single cKIT+ cells with DIA and iDIA. Both methods operated DIA MS2 scans at 60 ms max IIT, 20 m/z DIA windows and 20 W with a loop control of 0.6 seconds. iDIA replaced 2 or 3 DIA windows for each of 34 peptides per cycle with wwPRM scans. (**C**) Peptides identified in 0, 1, 5 and 10 cKIT+ cells, Median and Mad displayed.

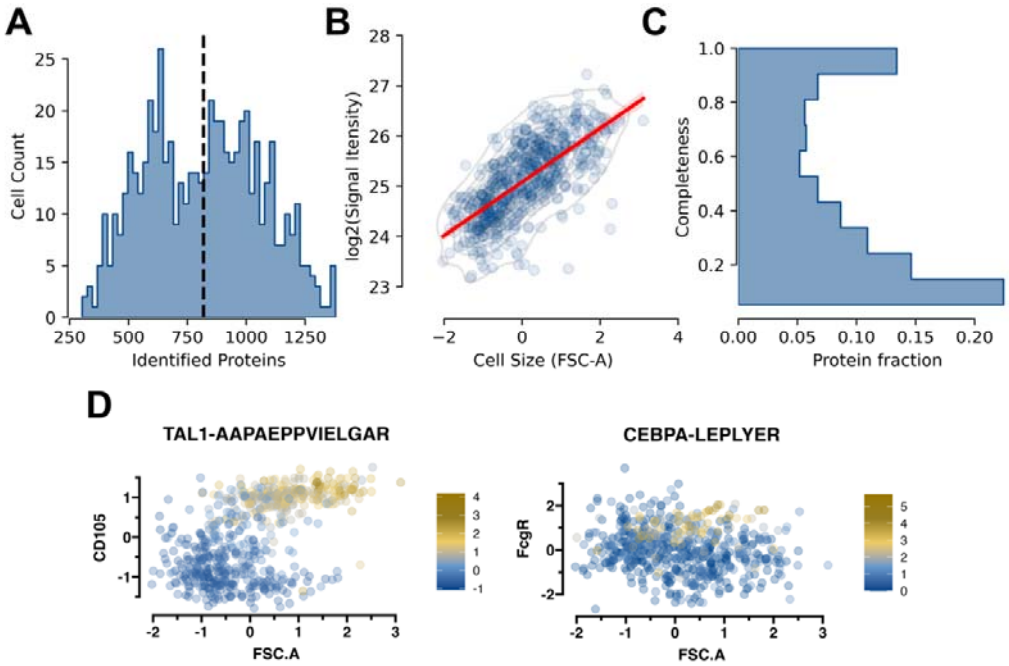

Supplementary Figure 6 580 single cKIT+ cells acquired with iDIA (**A**) Number of proteins identified per cell. Dashed line shows median (**B**) Correlation of cell size based on FSC-A and log2(MS1 signal intensity) (**C**) Protein completeness across all cells (**D**) correlation of FSC-A with FACs marker. Z-scored TF peptide expression is illustrated in color.

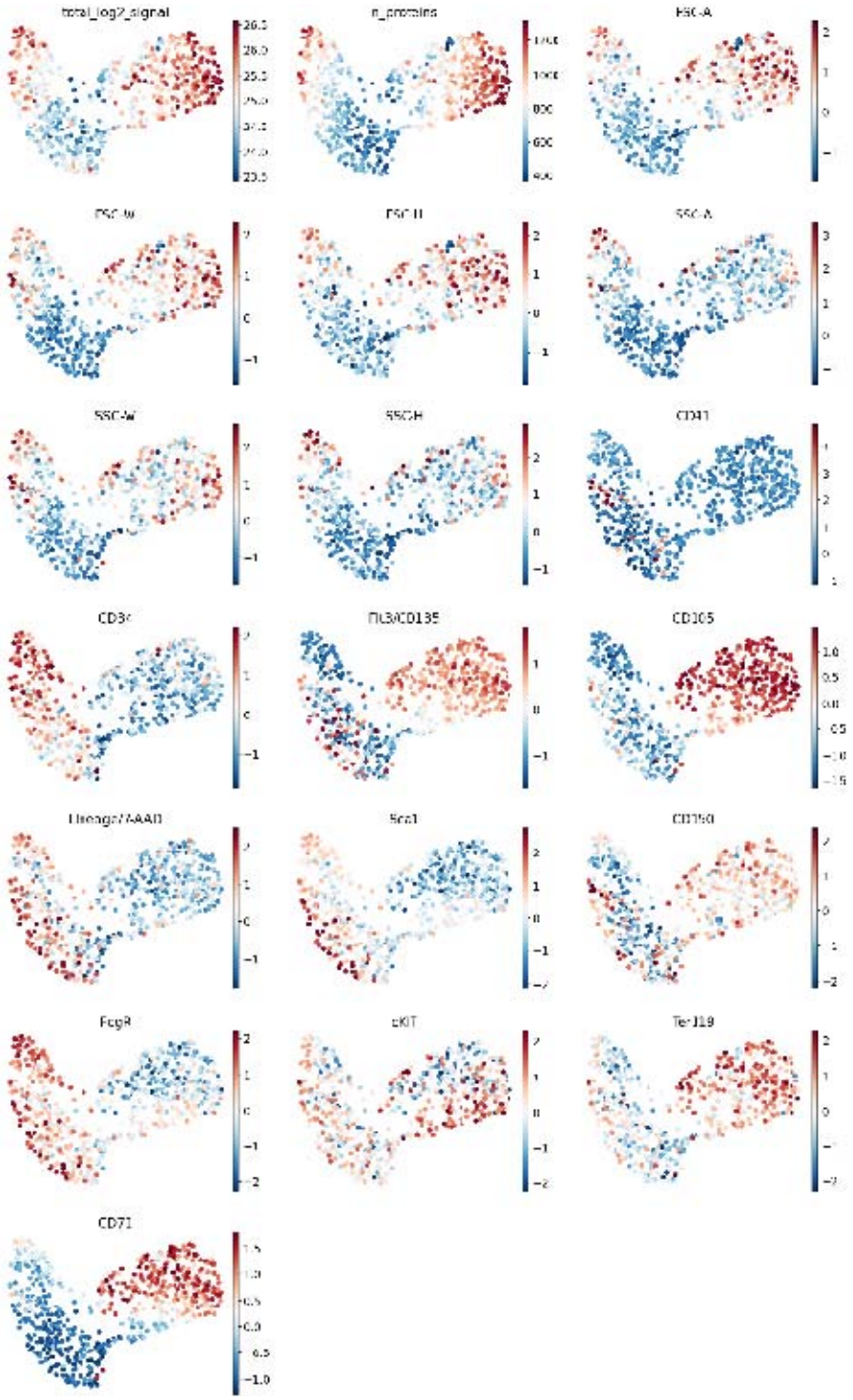

Supplementary Figure 7 580 single cKIT+ cells acquired with iDIA. UMAP embedding based on global cell proteome illustrating FACS marker expression.

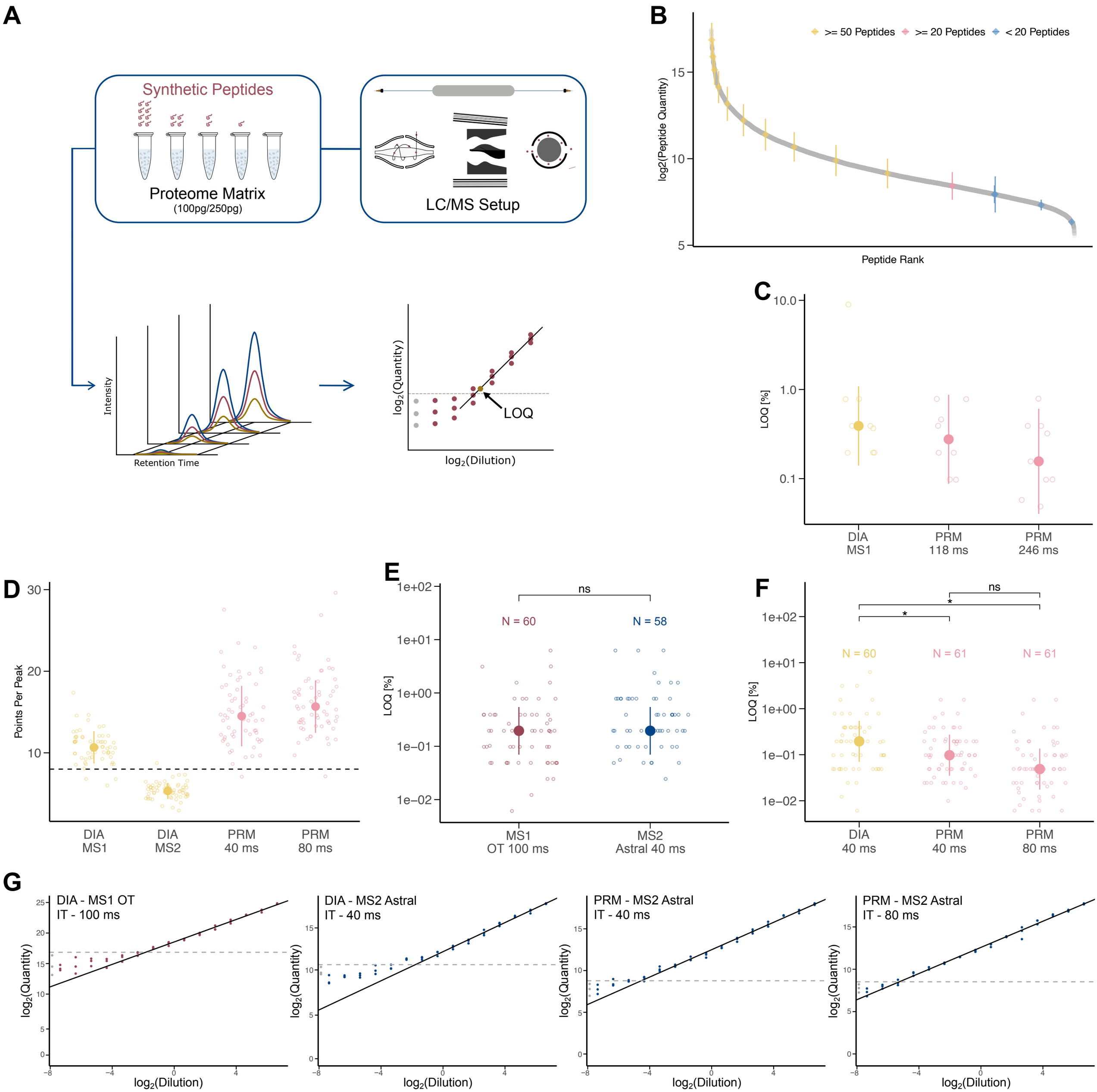
A
Synthetic Peptides
Proteome Matrix
(100pg/250pg)
LC/MS Setup
Intensity
Retention Time
log2(Quantity)
LOQ
log2(Dilution)
B
>= 50 Peptides
>= 20 Peptides
< 20 Peptides
log2(Peptide Quantity)
Peptide Rank
C
LOQ [%]
DIA MS1
PRM 118 ms
PRM 246 ms
D
Points Per Peak
DIA MS1
DIA MS2
PRM 40 ms
PRM 80 ms
E
ns
N = 60
N = 58
LOQ [%]
MS1 OT 100 ms
MS2 Astral 40 ms
F
ns
*
*
N = 60
N = 61
N = 61
LOQ [%]
DIA 40 ms
PRM 40 ms
PRM 80 ms
G
DIA - MS1 OT
IT - 100 ms
DIA - MS2 Astral
IT - 40 ms
PRM - MS2 Astral
IT - 40 ms
PRM - MS2 Astral
IT - 80 ms
log2(Quantity)
log2(Dilution)

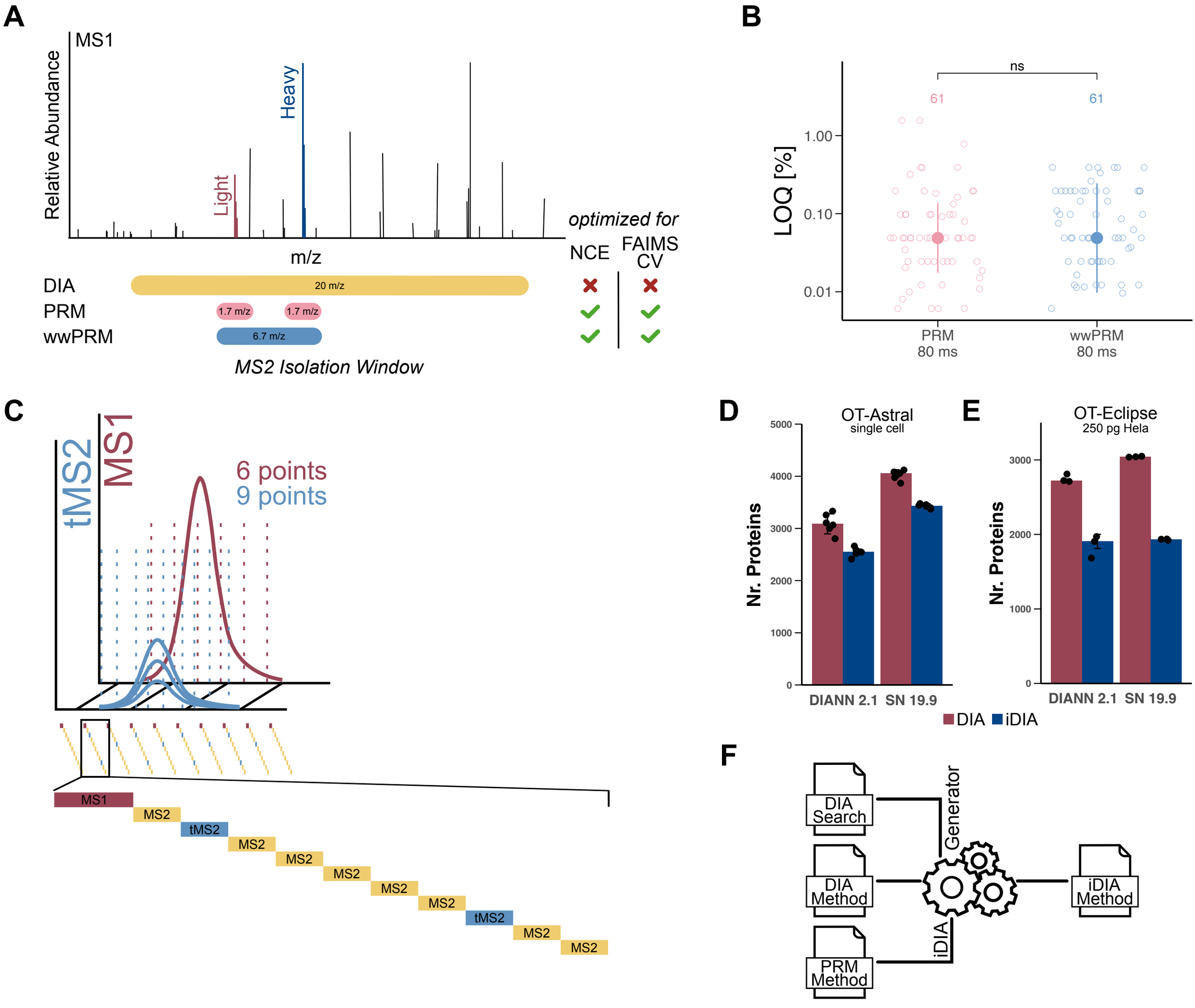
A
MS1
Relative Abundance
Heavy
Light
m/z
optimized for
NCE
FAIMS CV
DIA
20 m/z
PRM
1.7 m/z
1.7 m/z
wwPRM
6.7 m/z
MS2 Isolation Window
B
ns
61
61
LOQ [%]
1.00
0.10
0.01
PRM 80 ms
wwPRM 80 ms
C
tMS2
MS1
6 points
9 points
MS1
MS2
tMS2
MS2
MS2
MS2
MS2
MS2
tMS2
MS2
MS2
D
OT-Astral
single cell
Nr. Proteins
5000
4000
3000
2000
1000
0
DIANN 2.1
SN 19.9
E
OT-Eclipse
250 pg Hela
Nr. Proteins
3000
2000
1000
0
DIANN 2.1
SN 19.9
DIA
iDIA
F
DIA Search
DIA Method
PRM Method
Generator
iDIA
iDIA Method

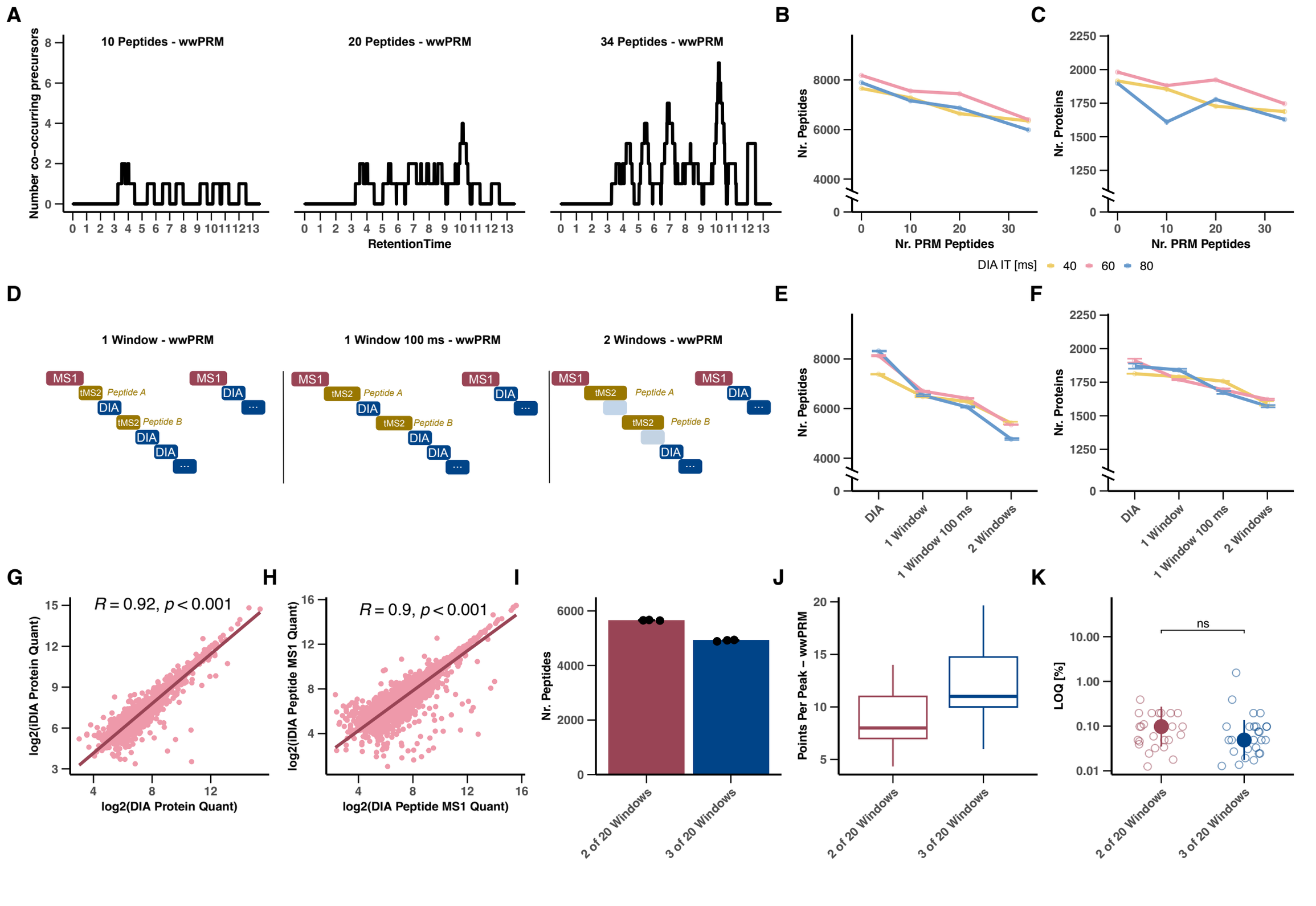
A
10 Peptides - wwPRM
20 Peptides - wwPRM
34 Peptides - wwPRM
Number co-occurring precursors
RetentionTime
B
Nr. Peptides
Nr. PRM Peptides
C
Nr. Proteins
Nr. PRM Peptides
DIA IT [ms] 40 60 80
D
1 Window - wwPRM
1 Window 100 ms - wwPRM
2 Windows - wwPRM
MS1
tMS2
Peptide A
Peptide B
DIA
E
Nr. Peptides
F
Nr. Proteins
DIA
1 Window
1 Window 100 ms
2 Windows
G
R = 0.92, p < 0.001
log2(iDIA Protein Quant)
log2(DIA Protein Quant)
H
R = 0.9, p < 0.001
log2(iDIA Peptide MS1 Quant)
log2(DIA Peptide MS1 Quant)
I
Nr. Peptides
2 of 20 Windows
3 of 20 Windows
J
Points Per Peak – wwPRM
2 of 20 Windows
3 of 20 Windows
K
ns
LOQ [%]
2 of 20 Windows
3 of 20 Windows

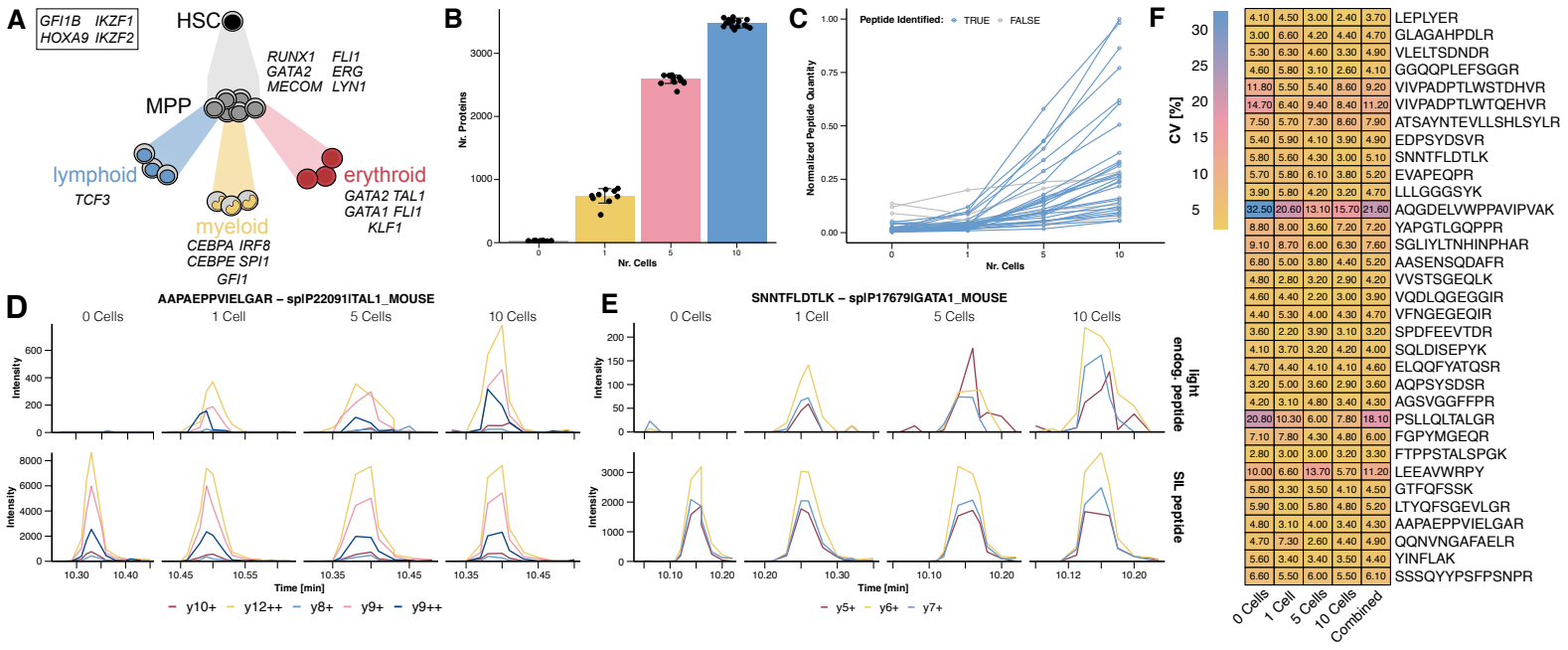
A
GFI1B IKZF1
HOXA9 IKZF2
HSC
RUNX1 FLI1
GATA2 ERG
MECOM LYN1
MPP
lymphoid
TCF3
myeloid
CEBPA IRF8
CEBPE SPI1
GFI1
erythroid
GATA2 TAL1
GATA1 FLI1
KLF1
B
Nr. Proteins
Nr. Cells
C
Peptide Identified: TRUE FALSE
Normalized Peptide Quantity
Nr. Cells
D
AAPAEPPVIELGAR – sp|P22091|TAL1_MOUSE
0 Cells
1 Cell
5 Cells
10 Cells
Intensity
Time [min]
y10+ y12++ y8+ y9+ y9++
E
SNNTFLDTLK – sp|P17679|GATA1_MOUSE
0 Cells
1 Cell
5 Cells
10 Cells
Intensity
Time [min]
y5+ y6+ y7+
light peptide
SIL peptide
F
CV [%]
LEPLYER 4.10 4.50 3.00 2.40 3.70
GLAGAHPDLR 3.00 6.60 4.20 4.40 4.70
VLELTSDNDR 5.30 6.30 4.60 3.30 4.90
GGQQPLEFSGGR 4.60 5.80 3.10 2.60 4.10
VIVPADPTLWSTDHVR 11.80 5.50 5.40 8.60 9.20
VIVPADPTLWTQEHVR 14.70 6.40 9.40 8.40 11.20
ATSAYNTEVLLSHLSYLR 7.50 5.70 7.30 8.60 7.90
EDPSYDSVR 5.40 5.90 4.10 3.90 4.90
SNNTFLDTLK 5.80 5.60 4.30 3.00 5.10
EVAPEQPR 5.70 5.80 6.10 3.80 5.20
LLLGGGSYK 3.90 5.80 4.20 3.20 4.70
AQGDELVWPPAVIPVAK 32.50 20.60 13.10 15.70 21.60
YAPGTLGQPPR 8.80 8.00 3.60 7.20 7.20
SGLIYLTNHINPHAR 9.10 8.70 6.00 6.30 7.60
AASENSQDAFR 6.80 5.00 3.80 4.40 5.20
VVSTSGEQLK 4.80 2.80 3.20 2.90 4.20
VQDLQGEGGIR 4.60 4.40 2.20 3.00 3.90
VFNGEGEQIR 4.40 5.30 4.00 4.30 4.70
SPDFEEVTDR 3.60 2.20 3.90 3.10 3.20
SQLDISEPYK 4.10 3.70 3.20 4.20 4.00
ELQQFYATQSR 4.70 4.40 4.10 4.10 4.60
AQPSYSDSR 3.20 5.00 3.60 2.90 3.60
AGSVGGFFPR 4.20 3.10 4.80 3.40 4.30
PSLLQLTALGR 20.80 10.30 6.00 7.80 18.10
FGPYMGEQR 7.10 7.80 4.30 4.80 6.00
FTPPSTALSPGK 2.80 3.00 3.00 3.20 3.30
LEEAVWRPY 10.00 6.60 13.70 5.70 11.20
GTFQFSSK 5.80 3.30 3.50 4.10 4.50
LTYQFSGEVLGR 5.90 3.00 5.80 4.80 5.20
AAPAEPPVIELGAR 4.80 3.10 4.00 3.40 4.30
QQNVNGAFAELR 4.70 7.30 2.60 4.40 4.90
YINFLAK 5.60 3.40 3.40 3.50 4.40
SSSQYYPSFPSNPR 6.60 5.50 6.00 5.50 6.10
0 Cells
1 Cell
5 Cells
10 Cells
Combined

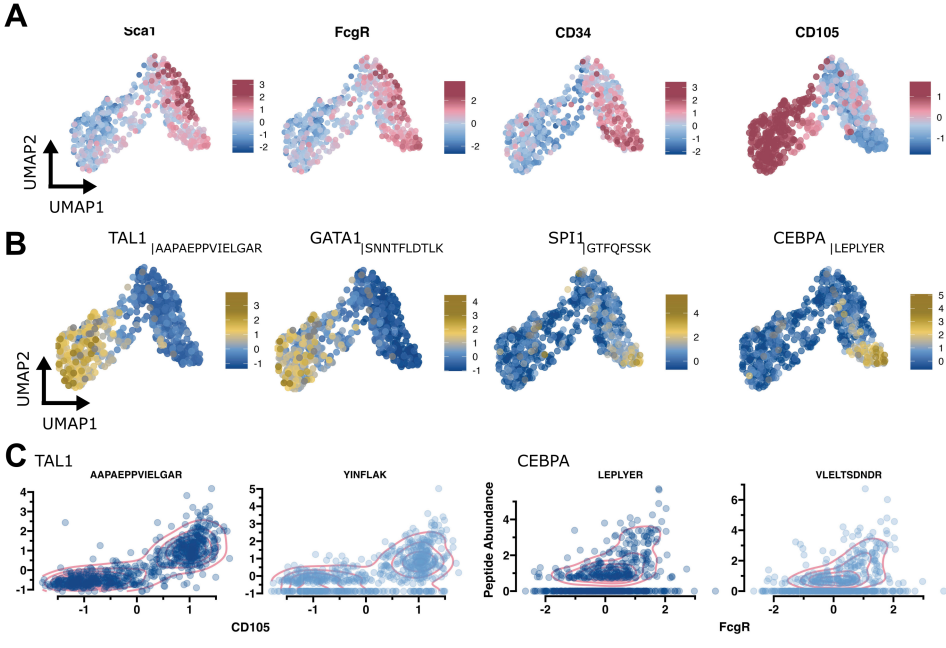
A
Sca1
FcgR
CD34
CD105
UMAP2
UMAP1
B
TAL1 |AAPAEPPVIELGAR
GATA1 |SNNTFLDTLK
SPI1 |GTFQFSSK
CEBPA |LEPLYER
UMAP2
UMAP1
C
TAL1
AAPAEPPVIELGAR
YINFLAK
CEBPA
LEPLYER
VLELTSDNDR
Peptide Abundance
CD105
FcgR